

The Tuscarora Au-Ag District: Eocene Volcanic-Hosted Epithermal Deposits in the Carlin Gold Region, Nevada

STEPHEN B. CASTOR,[†]

Nevada Bureau of Mines and Geology, University of Nevada, Reno, Reno, Nevada 89557

DAVID R. BODEN,

1445 High Chaparral Drive, Reno, Nevada 89511

CHRISTOPHER D. HENRY,

Nevada Bureau of Mines and Geology, University of Nevada, Reno, Reno, Nevada 89557

JEAN S. CLINE,

Geoscience Department, University of Nevada, Las Vegas, Nevada 89154-4010

ALBERT H. HOFSTRA,

U.S. Geological Survey, Denver Federal Center, Box 25046, Denver, Colorado 80225

WILLIAM C. MCINTOSH,

New Mexico Bureau of Geology, New Mexico Institute of Mining and Technology, Socorro, New Mexico 87801

RICHARD M. TOSDAL,

Mineral Deposit Research Unit, Department of Earth and Ocean Sciences, University of British Columbia, 6339 Stores Road, Vancouver, British Columbia, Canada V6T 1Z4

AND JOSEPH P. WOODEN

U.S. Geological Survey, 345 Middlefield Road, Menlo Park, California 94025

Abstract

The Tuscarora mining district contains the oldest and the only productive Eocene epithermal deposits in Nevada. The district is a particularly clear example of association of low-sulfidation deposits with igneous activity and structure, and it is unusual in that it consists of two adjoining but physically and chemically distinct types of low-sulfidation deposits. Moreover, Tuscarora deposits are of interest because they formed contemporaneously with nearby, giant Carlin-type gold deposits. The Tuscarora deposits formed within the 39.9 to 39.3 Ma Tuscarora volcanic field, along and just outside the southeastern margin of the caldera-like Mount Blitzen volcanic center. Both deposit types formed at 39.3 Ma, contemporaneous with the only major intrusive activity in the volcanic field. No deposits are known to have formed during any of the intense volcanic phases of the field. Intrusions were the apparent heat source, and structures related to the Mount Blitzen center were conduits for hydrothermal circulation. The ore-forming fluids interacted dominantly with Eocene igneous rocks.

The two deposit types occur in a northern silver-rich zone that is characterized by relatively high Ag/Au ratios (110–150), narrow alteration zones, and quartz and carbonate veins developed mostly in intrusive dacite, and in a southern gold-rich zone that is typified by relatively low Ag/Au ratios (4–14), more widespread alteration, and quartz-fissure and stockwork veins commonly developed in tuffaceous sedimentary rocks. The deposit types have similar fluid inclusion and Pb and S isotope characteristics but different geochemical signatures. Quartz veins from both zones have similar thermal and paragenetic histories and contain fluid inclusions that indicate that fluids cooled from between 260° and 230°C to less than 200°C. Fluid boiling may have contributed to precious-metal deposition. Veins in both zones have relatively high As and Sb and low Bi, Te, and W. The silver zone has high Ca, Pb, Mn, Zn, Cd, Tl, and Se. The gold zone has high Hg and Mo. A few samples from an area of overlap between the two zones share chemical characteristics of both deposit types. The deposit types could represent a single zoned or evolving system in which hydrothermal fluids rose along structures within the silver zone, preferentially deposited Ag and base metals, and then spread into the gold zone. Alternatively, the deposit types could represent two distinct but temporally indistinguishable hydrothermal cells that only narrowly overlapped spatially.

[†]Corresponding author: e-mail, scastor@unr.edu

As noted in previous studies, the hydrothermal fluids that generated the Tuscarora and other epithermal deposits could have evolved from Carlin-type fluids by boiling and mixing with meteoric water. If so, the Tuscarora deposit may represent epithermal conditions above Carlin-type deposits, and Carlin-type deposits may lie beneath the district.

Introduction

THE TUSCARORA mining district produced 204,000 oz Au (6,345 kg) and 7,600,000 oz Ag (236,000 kg) during several periods of mining between 1867 and 1990 (Table 1). Despite this modest production, volcanic-hosted, epithermal Au-Ag deposits in the district are significant because they are the oldest epithermal deposits in Nevada and the only significant Eocene deposits of that type. The Tuscarora deposits are unusual in that they consist of two geochemically distinct but contiguous low-sulfidation types, one with relatively high Ag/Au ratios and moderate base metals and another with low Ag/Au ratios and negligible base metals. Their spatial and temporal association with the Tuscarora volcanic field, the largest Eocene volcanic field in Nevada, is particularly clear. Eocene igneous centers are widespread in northeastern Nevada and northwestern Utah (Fig. 1), and numerous major metal deposits are associated with them. Examples include the Cu and Au deposits of Bingham Canyon and Battle Mountain (Babcock et al., 1995; Theodore, 2000), base metal- and Ag-bearing skarn at Ward (Hasler et al., 1991), Au skarn at McCoy (Brooks et al., 1991; Johnston, 2000), and porphyry Mo at Mount Hope (Westra and Riedell, 1996). In addition, it is now well established that most Carlin-type gold deposits of the region formed in the Eocene, generally between 42 and 36 Ma (Arehart et al., 1993; Thorman et al., 1995; Emsbo et al., 1996; Leonardson and Rahn, 1996; Phinisey et al., 1996; Groff et al., 1997; Hall et al., 1997, 2000; Teal and Jackson, 1997; Hofstra et al., 1999; Hofstra and Cline, 2000; Johnston, 2000; Ressel et al., 2000a, b; Tretbar et al., 2000; Cline, 2001). Eocene magmatism has been proposed as the heat source for hydrothermal systems that generated Carlin-type deposits (Henry and Boden, 1998b; Henry and Ressel, 2000; Ressel et al., 2000a), although this proposal continues to be debated (Ilchik and Barton, 1997; Hofstra and Cline, 2000).

In this paper new data on the timing of mineralization, chemistry, mineral assemblages, fluid inclusions, and isotopic patterns at Tuscarora are used to evaluate the relationship between igneous activity and mineralization, between high Ag/Au and low Ag/Au deposits in the Tuscarora district, and

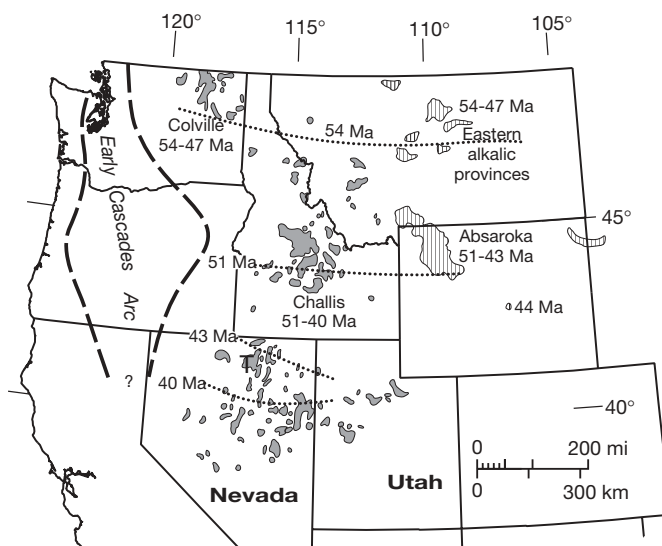


FIG. 1. Regional geologic setting of Tuscarora (T) within Eocene igneous provinces of the northwestern United States (from Stewart and Carlson, 1978; Seedorff, 1991; Christiansen and Yeats, 1992; Hiza and Grunder, 1997; Henry and Ressel, 2000).

between Tuscarora epithermal mineralization and Carlin-type deposits. Previously, little was known about the Eocene geology of the region (Brooks et al., 1995a, b) or about the Tuscarora district, although Emmons (1910) and Nolan (1936) identified the apparent juxtaposition of the two deposit types. On the basis of two reconnaissance studies (Berger et al., 1991; Boden et al., 1993), the Tuscarora volcanic field was identified as Eocene and apparently the largest volcanic field of this age in the Great Basin. The origin and age of Carlin-type deposits were unknown, but an Eocene age was considered likely (Thorman et al., 1995). Because the Tuscarora district lies between the Carlin trend, the largest concentration of Carlin-type deposits in the world, and other major Carlin-type deposits at Jerritt Canyon (Fig. 2), an understanding of Eocene magmatism, tectonics, and mineralization at Tuscarora may help understand Carlin-type deposits. Detailed geologic mapping of the Tuscarora volcanic field and district (Henry and Boden, 1998a; Henry and Boden, 1999; Henry et al., 1999) provides the necessary geologic framework.

Regional Setting: Eocene Magmatism in Northeastern Nevada

The Tuscarora volcanic field is part of a broad area of Eocene (~43–34 Ma) magmatism that occurred throughout northeastern Nevada and northwestern Utah (Fig. 1). Regionally, igneous centers in Nevada and Utah are a continuation of a southward sweep of early Cenozoic magmatism that began in British Columbia and Washington (Christiansen and

TABLE 1. Production from the Tuscarora Mining District

Period	Source	Au (oz)	Ag (oz)	Other (lb)
1876–1895	Silver zone	150,000 ¹	7,000,000	
1898–1903	Dexter mine	40,000	100,000	
1903–1941	Various	18,000	200,000	Pb: 145,000 Cu: 10,000 ²
1979–1981	Leaching of dumps	2,000	147,000	
1987–1990	Dexter mine	34,000	185,000	
Total		204,000	7,632,000	

Based on data in Nolan (1936), LaPointe et al. (1991), and Crawford (1992)

¹ Includes 34,000 oz from placer mining

² Probably not from Tuscarora

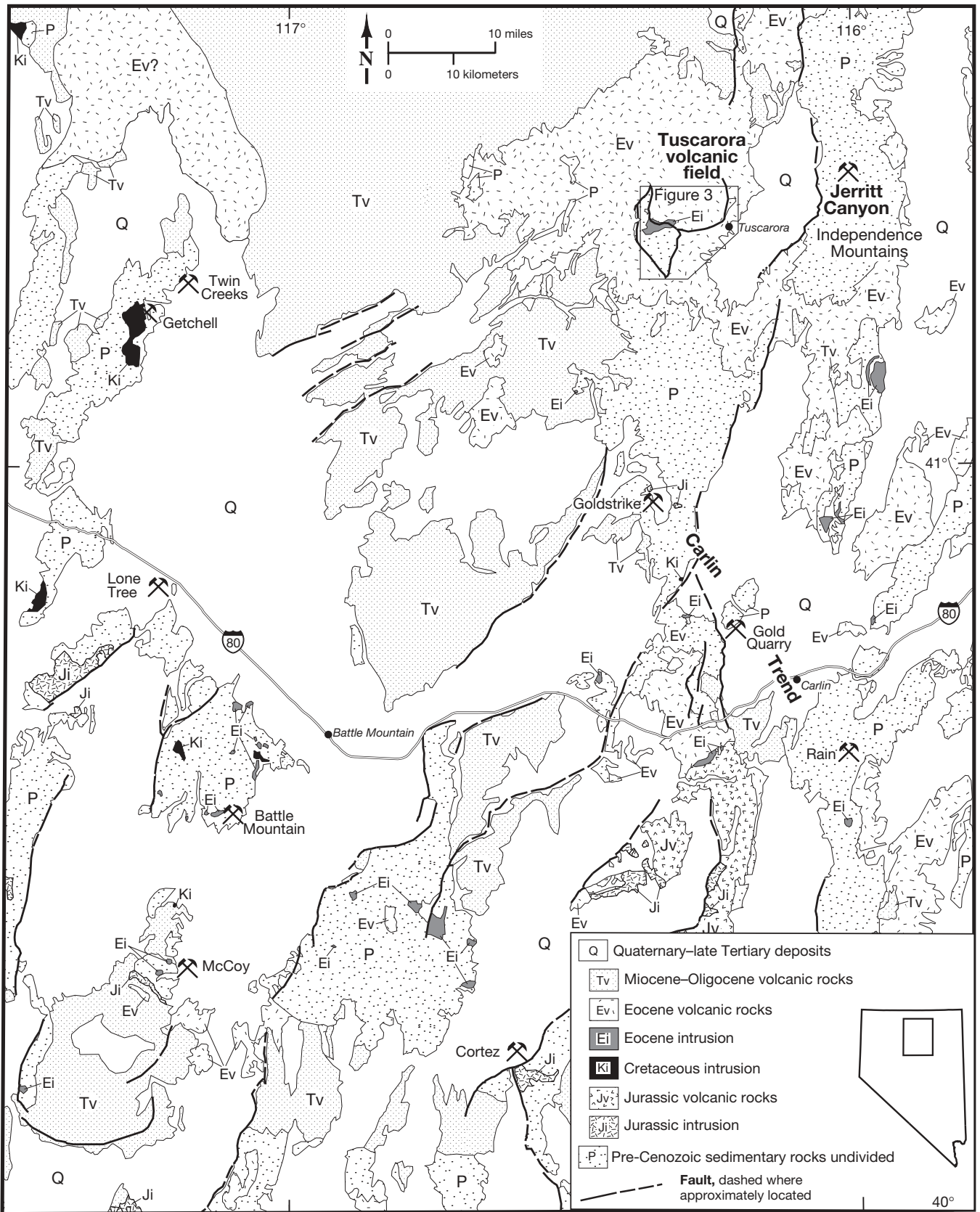


FIG. 2. Generalized geologic map of a part of northern Nevada (from Stewart and Carlson, 1978) that shows the largest Eocene volcanic centers of the region, most Carlin-type deposits, and other precious-metal deposits related to Eocene igneous centers.

Yeats, 1992). The Colville igneous complex of Washington (McCarley Holder et al., 1990; Carlson et al., 1991; Hooper et al., 1995) and the Challis volcanic field of Idaho (McIntyre et al., 1982; Janecke et al., 1997) represent earlier, northern parts of this magmatism. Igneous activity in the Colville complex began about 54 Ma, was most intense until about 50 Ma, and continued until 47 Ma (McCarley Holder et al., 1990). Magmatism in the Challis field began about 51 Ma and was most intense until about 44 Ma; waning volcanism continued until about 40 Ma (McIntyre et al., 1982). Eocene magmatism in northeastern Nevada and northern Utah began at 43 Ma (Brooks et al., 1995a, b) and was concentrated between 41 and 36 Ma (Brooks et al., 1995a, b; Henry and Boden, 1998b; Henry and Ressel, 2000; Ressel et al., 2000a; Theodore, 2000). Progressively younger magmatism continued farther south in Nevada at least into the early Miocene.

Eocene igneous rocks from Washington to Nevada are similar in composition (Henry and Ressel, 2000). The most abundant rocks are andesitic to dacitic lavas or granodiorite. More silicic rocks, such as rhyolite ash-flow tuffs or granite, are also present and locally voluminous. The rocks are moderately alkalic and notably potassic.

Geology of the Tuscarora Volcanic Field

The Tuscarora volcanic field is the largest (~2,000 km²) and probably the most diverse and complex Eocene volcanic field in Nevada (Figs. 2 and 3; Berger et al., 1991; Boden et al., 1993; Henry and Boden, 1998a, 1999; Henry et al., 1998, 1999). The Tuscarora volcanic field underwent six major pulses of activity in a brief but intense period between about 39.9 and 39.3 Ma (Table 2). Additionally, rhyolite lavas and dikes were emplaced at about 35 Ma in the western part of the field. From oldest to youngest, the six pulses produced (1) early rhyolitic to dacitic ash-flow tuffs in the western part of the field (39.9 Ma), (2) andesitic to dacitic lava flows and tuffaceous sedimentary rocks of the Pleasant Valley volcanic complex (39.9–39.7 Ma), (3) dacitic domes, small-volume pyroclastic-flow deposits, and epiclastic deposits of the Mount Blitzen volcanic center (39.8–39.7 Ma), (4) rhyolitic ash-flow tuff of the Big Cottonwood Canyon caldera (39.7 Ma), (5) a granodiorite pluton and andesitic to rhyolitic dikes and small intrusions of the Mount Neva intrusive episode (39.5–39.3 Ma), and (6) andesitic to dacitic lava flows of Sixmile Canyon (39.3 Ma). Gold-silver mineralization in the Tuscarora district occurred at about 39.3 Ma, contemporaneous with the Mount Neva intrusions during the last phases of magmatism.

Prevolcanic rocks

The Tuscarora volcanic field formed in an area of complexly deformed lower Paleozoic rocks that constitute the upper plate of the Roberts Mountains allochthon (Roberts, 1964). Two mappable packages of Paleozoic rocks crop out in the Tuscarora volcanic field (Fig. 3). A northern package (Pzq), which includes a wedge of Ordovician and Silurian rocks immediately north of the Tuscarora district, consists of quartzite, siltstone, chert, and minor limestone (Coats, 1987; Henry and Boden, 1998a). A southern Silurian and Devonian package (Pzc) consists of siltstone and chert, and minor sandstone and limestone. Carbonate-bearing, lower-plate rocks, major hosts for gold deposits in the Carlin trend and

Independence Mountains, do not crop out in the Tuscarora volcanic field but should underlie the upper-plate rocks.

Early ash-flow tuffs

The oldest Tertiary volcanic rocks are 39.9 to 39.8 Ma rhyolitic to dacitic ash-flow tuffs that crop out mostly in the western part of the Tuscarora volcanic field, west of the area shown on Figure 3 (Table 2). The youngest dacitic tuff is probably related to the Pleasant Valley volcanic complex, but sources for the other tuffs are unknown.

Pleasant Valley volcanic complex

The Pleasant Valley volcanic complex consists of andesitic to dacitic lavas (Tp) and lava domes (Tpd), shallow intrusions, and tuff and volcanoclastic sedimentary rocks that crop out extensively in the southern part of the field. Sources for the volcanic material include several lava domes, shallow intrusions, and a pyroclastic center in the southwestern and southern parts of the complex. Lavas total as much as 500 m in thickness in the central part of their outcrop but become increasingly interbedded with volcanoclastic deposits northeastward toward Tuscarora, where mostly fine-grained volcanoclastic rocks are abundant and a major ore host. ⁴⁰Ar/³⁹Ar ages constrain Pleasant Valley activity to about 39.9 to 39.7 Ma (Fig. 4 and Table 2).

Mount Blitzen volcanic center

The Mount Blitzen center is a large (11 × 6 km), fault-bounded basin filled with dacitic intrusive and extrusive rocks and having many characteristics of a caldera. The basin is truncated on the north by the younger Big Cottonwood Canyon caldera; its original extent in that direction is unknown. The center is filled with a thick sequence of dacitic domes (Tbd) and the dacitic tuff of Mount Blitzen (Tbt), which consists of small-volume pyroclastic-flow and epiclastic deposits. Pyroclastic rocks are petrographically similar to rocks in the domes and are in part block and ash flows erupted from them. Epiclastic rocks consist mostly of reworked, very coarse to fine fragments of the primary volcanic rocks. Both pyroclastic and epiclastic rocks contain megabreccia blocks of the dacitic domes, older andesite probably of the Pleasant Valley complex and, rarely, Paleozoic rocks that were shed from the margins of the center. The composite tuff of Mount Blitzen is about 4 km thick where exposed in the eastern limb of an anticline through the Mount Blitzen center. The center formed between about 39.8 and 39.7 Ma on the basis of ⁴⁰Ar/³⁹Ar ages on the older Pleasant Valley volcanic complex and the younger Big Cottonwood Canyon caldera (Fig. 4 and Table 2).

Big Cottonwood Canyon caldera

The Big Cottonwood Canyon caldera is a large, rhyolitic caldera that lies north of and truncates the Mount Blitzen volcanic center (Fig. 3). The caldera margin is marked by the juxtaposition of the thick intracaldera tuff of Big Cottonwood Canyon (Tct) against Paleozoic rocks and tuff of Mount Blitzen. The caldera is at least 15 km across and extends northward outside the mapped area. Tuff near the caldera margin contains debris lenses and megabreccia blocks of andesite, tuff of Mount Blitzen, and Paleozoic rocks up to

TABLE 2. $^{40}\text{Ar}/^{39}\text{Ar}$ Ages of Tertiary Igneous Rocks and Mineralization, Tuscarora Volcanic Field

Sample location and number	Rock type	North latitude	West longitude	Mineral	Age method	<i>n</i>	^{39}Ar (%)	Age (Ma)	$\pm 1\sigma$
Mineralized rock of the Tuscarora district									
H96-98	Dexter zone	41°18.7'	116°13.6'	Adularia	Plateau		90.5	39.25	0.07
H96-93	Modoc vein	41°18.4'	116°15.2'	Adularia	Plateau		96.4	39.28	0.08
H96-99	North-northwest vein at Dexter pit	41°18.3'	116°13.3'	Adularia	Plateau		82.5	39.24	0.09
H96-102	Grand Prize vein	41°19.2'	116°13.2'	Adularia	Plateau		99.7	39.27	0.07
H96-104	Navajo vein, North Commonwealth mine	41°19.4'	116°14.1'	Adularia	Plateau		91.6	39.32	0.07
H96-45	Castile Mountain alteration	41°16.9'	116°16.5'	Adularia	Plateau		88.7	39.14	0.07
Lavas of Sixmile Canyon									
DB-3	Dacite lava (Tsd)	41°21.4'	116°12.1'	Hornblende	Plateau		59.6	39.25	0.16
Rhyolite of Walker Mountain									
H96-65	Porphyritic rhyolite dike	41°22.5'	116°19.4'	Sanidine	Single crystal	12		33.77	0.05
H96-59	Porphyritic rhyolite lava dome	41°22.5'	116°19.4'	Sanidine	Single crystal	15		35.05	0.05
H97-85	Porphyritic rhyolite lava	41°17.6'	116°28.3'	Sanidine	Single crystal	15		35.15	0.05
DB-19	Porphyritic rhyolite lava	41°19.3'	116°23.2'	Sanidine	Single crystal	15		35.29	0.05
Mount Neva intrusive episode									
Late dikes									
H96-19	Porphyritic rhyolite (Tmr)	41°22.4'	116°14.9'	Sanidine	Single crystal	15		39.34	0.04
				Hornblende	Plateau		93.1	39.46	0.15
					Integrated age		100	39.2	0.2
				Plagioclase	Plateau		65.8	39.17	0.11
DB-35	Porphyritic dacite	41°18.6'	116°17.5'	Hornblende	Plateau		63.2	39.51	0.18
DB-43	Quartz-phyric porphyritic dacite	41°18.1'	116°17.1'	Hornblende	Single step		84.9	39.37	0.12
Mount Neva pluton									
H96-72A	Granodiorite	41°19.3'	116°21.6'	Biotite	Plateau		58.7	39.37	0.14
				Biotite	Integrated age		100	39.6	0.3
Early porphyritic dacite (Tmd)									
H96-63		41°21.3'	116°21.3'	Hornblende	Plateau		92.6	39.58	0.20
H96-103		41°19.0'	116°13.6'	Hornblende	Plateau		77.2	39.43	0.13
Big Cottonwood Canyon caldera									
Tuff of Big Cottonwood Canyon									
H96-42	Intracaldera tuff	41°22.4'	116°15.6'	Sanidine	Single crystal	15		39.67	0.05
H96-80	Intracaldera tuff, single pumice	41°24.5'	116°20.6'	Sanidine	Single crystal	13		39.67	0.05
96WC28	Outflow tuff	41°13.6'	116°32.3'	Sanidine	Single crystal	15		39.72	0.04
Mount Blitzen volcanic center									
DB-28	Tuff of Mount Blitzen (Tbt)	41°20.7'	116°21.5'	Biotite	Plateau		96.0	39.88	0.11
				Biotite	Integrated age		100	39.5	0.3
H96-92	Dacite of Mount Blitzen (Tbd)	41°19.1'	116°18.3'	Biotite	Plateau		83.8	39.40	0.07
				Biotite	Integrated age		100	39.03	0.18
Pleasant Valley volcanic complex									
H96-86	Hornblende andesite lava	41°16.2'	116°21.2'	Hornblende	Plateau		93.4	39.69	0.14
H96-73	Hornblende andesite lava	41°15.4'	116°19.9'	Hornblende	Plateau		97.8	39.86	0.12
Early tuffs									
H96-32	Tuff of Sugarloaf Butte	41°13.4'	116°15.1'	Sanidine	Single crystal	15		39.84	0.05
H97-51	Vitric tuff	41°16.8'	116°27.6'	Plagioclase	Single crystal	39		39.75	0.25
H97-30	Tuff of Nelson Creek	41°16.4'	116°08.0'	Sanidine	Single crystal	16		39.92	0.06
H97-71	Tuff of Nelson Creek	41°15.1'	116°25.2'	Sanidine	Single crystal	12		39.88	0.06
H97-110	Tuff of Nelson Creek	41°15.8'	116°30.1'	Sanidine	Single crystal	9		39.97	0.06

Analytical methods in McIntosh and Chamberlin (1994); samples irradiated in Al discs for 7 h in D-3 position, Nuclear Science Center, College Station, Texas; neutron flux monitor Fish Canyon Tuff sanidine (FC-1); assigned age = 27.84 Ma (Deino and Potts, 1990) relative to Mmhb-1 at 520.4 Ma (Samson and Alexander, 1987); weighted mean $^{40}\text{Ar}/^{39}\text{Ar}$ ages calculated by the method of Samson and Alexander (1987)

Minerals separated from crushed, sieved samples by standard magnetic and density techniques; feldspar concentrates leached with dilute HF to remove matrix and hand-picked

Decay constants and isotopic abundances after Steiger and Jäger (1977)

n = number of single crystals analyzed; % ^{39}Ar = percentage of ^{39}Ar that defines plateau

several hundred meters in diameter. The age of ash-flow eruption and caldera collapse is tightly constrained by three sanidine $^{40}\text{Ar}/^{39}\text{Ar}$ ages that range from 39.67 ± 0.05 to 39.72 ± 0.05 Ma (Fig. 4 and Table 2).

Mount Neva intrusive episode

Major intrusive activity of the Tuscarora volcanic field is restricted to the Mount Neva episode, which developed in

three distinct pulses: early porphyritic dacite (Tmd), the Mount Neva granodiorite (Tmg), and late dikes (Tmi). All these rocks were emplaced into and immediately adjacent to the Mount Blitzen volcanic center (Fig. 3), between about 39.5 and 39.3 Ma (Fig. 4 and Table 2), and they are interpreted to be a late phase of activity of that center. Early dacites form numerous irregularly shaped intrusions along the western, southern, and eastern margins of the Mount

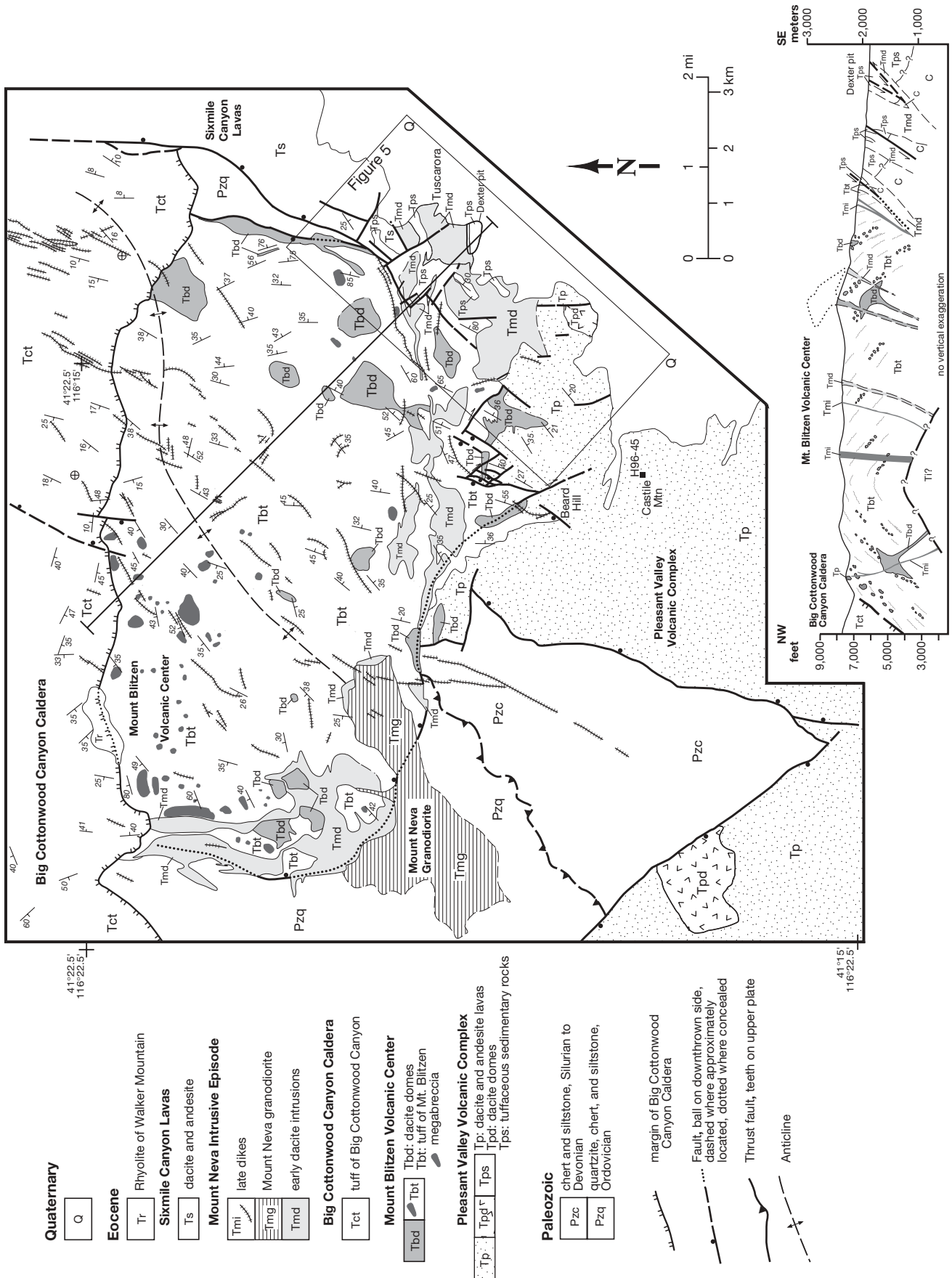


FIG. 3. Simplified geologic map and cross section of the Tuscarora volcanic field based on detailed mapping of Henry and Boden (1998a) and Henry et al. (1999).

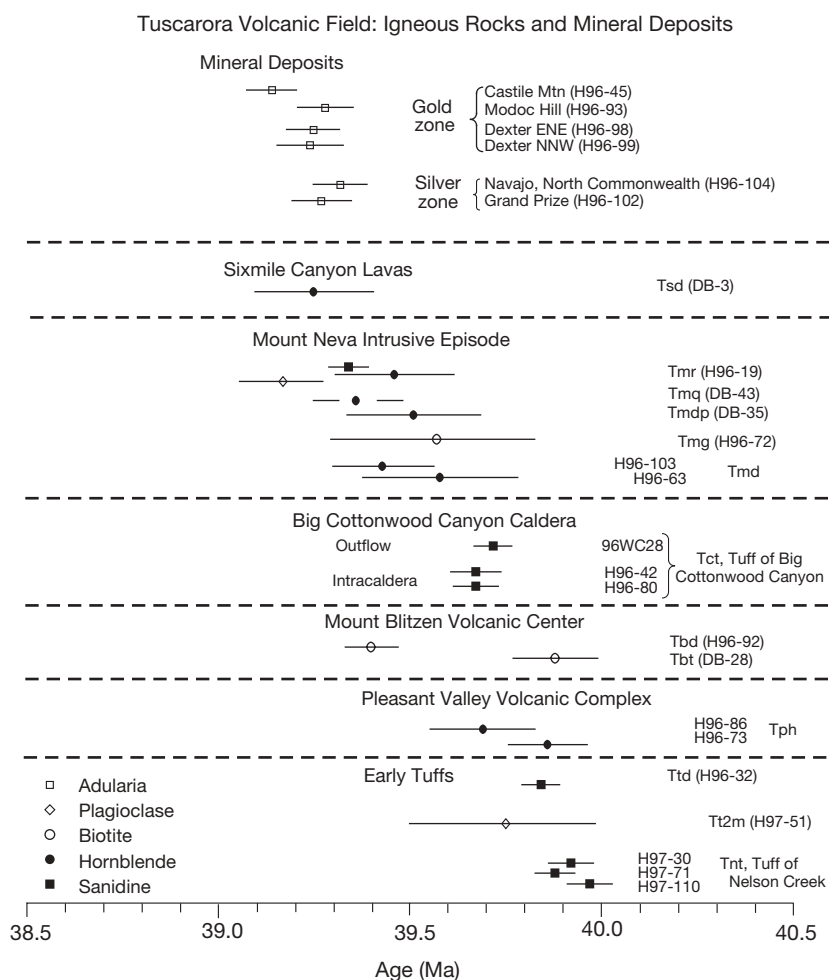


FIG. 4. $^{40}\text{Ar}/^{39}\text{Ar}$ ages (with 1 σ error bars) of igneous rocks and adularia in the Tuscarora volcanic field. Rocks are in stratigraphic order determined from field relations. Data listed in Table 1.

Blitzen volcanic center and a few dikes within the center. This distribution indicates that most intrusions rose along the faults that bound the center. Early dacite is abundant in the Tuscarora district, where it intrudes volcanoclastic sedimentary rocks of the Pleasant Valley complex, and is the other major host rock in the district.

The Mount Neva granodiorite (Tmg), the largest intrusion in the area, cuts the southwestern margin of the Mount Blitzen center. It is about 5 km \times 1 to 2 km, is elongate east-northeast, and has steep contacts with surrounding rocks.

Numerous late dikes, ranging from andesite to low-silica rhyolite, were the last manifestations of the Mount Neva episode. All the dikes form a broad, northeast-striking band through the middle of the Mount Blitzen center, parallel to and largely coinciding with the northeast-striking anticline. Several such dikes intruded early dacite or volcanoclastic rocks in the northwestern part of the Tuscarora district.

Sixmile Canyon lavas

Dacitic to andesitic lava flows and minor tuffs that crop out north of Tuscarora and east of the Big Cottonwood Canyon caldera are the youngest part of the Tuscarora volcanic field

(Ts; Fig. 3). Rock types are similar to those of the Pleasant Valley volcanic complex, but field relations and a $^{40}\text{Ar}/^{39}\text{Ar}$ date (39.25 ± 0.16 Ma; Table 2 and Fig. 4) demonstrate that they are younger. Compositional, petrographic, and age similarities suggest the lavas may be extrusive counterparts to late dacites of the Mount Neva intrusive episode.

35 Ma rhyolites

Rhyolitic volcanism resumed at about 35 Ma in the western part of the Tuscarora volcanic field. A rhyolite lava dome (Tr) was emplaced along the margin of the Big Cottonwood Canyon caldera, and rhyolite lavas erupted still farther southwest, outside the area shown in Figure 3.

Structure

The Tuscarora district sits along and just outside the Mount Blitzen volcanic center, and structures along the center's margin strongly influenced the location of mineralization (Figs. 3 and 5). The Mount Blitzen center is bounded by high-angle normal faults that separate the tuff of Mount Blitzen from older rocks outside the center. Restriction of the tuff to the center, the tuff's great thickness there, and megabreccia

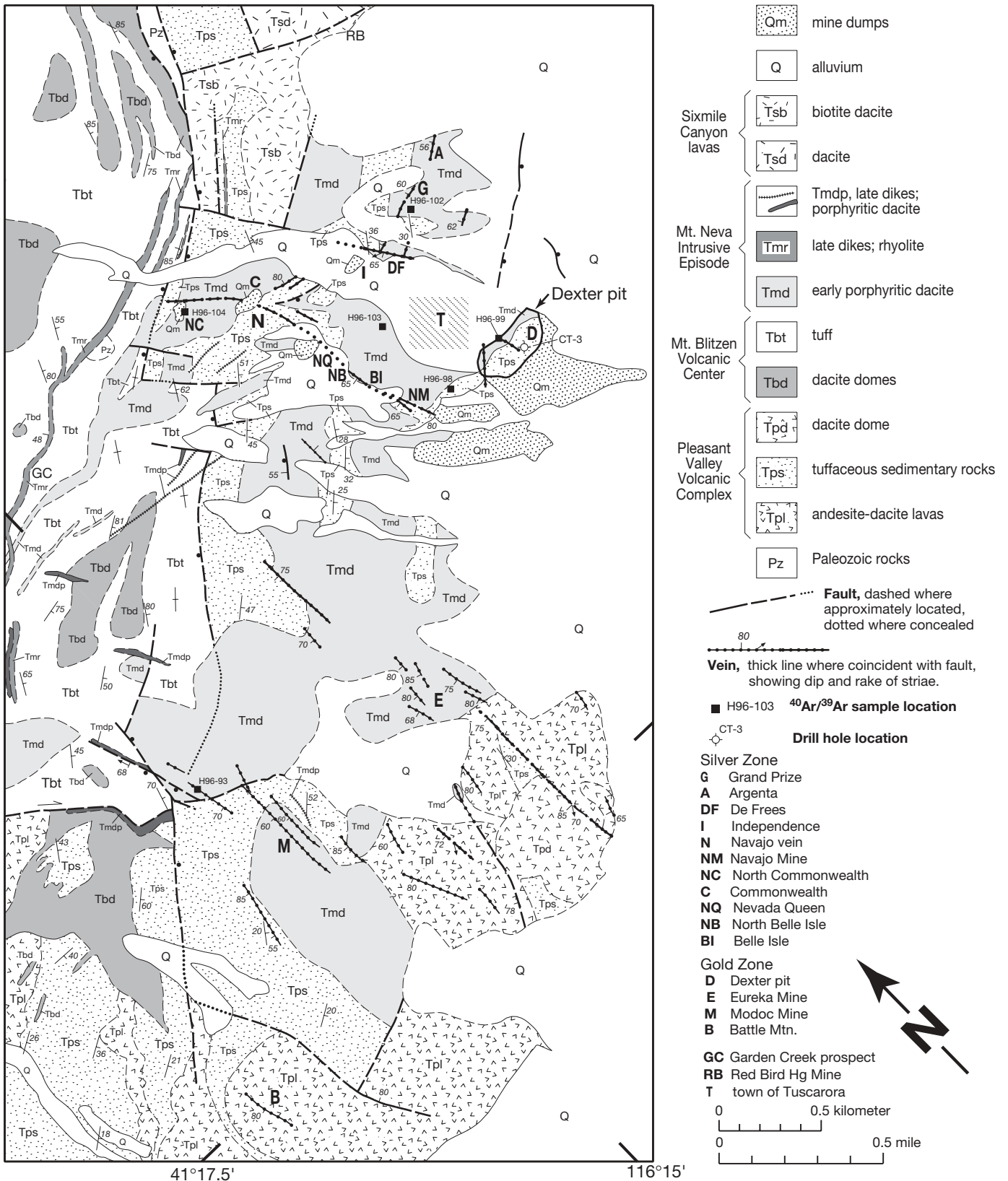


FIG. 5. Geologic map of the Tuscarora district; note that map is oriented northeast-southwest. Modified from Henry and Boden (1998) and Henry et al. (1999).

blocks incorporated into the tuff indicate simultaneous tuff deposition and subsidence of the center along these faults. The cumulative thickness of tuff exposed in the Mount Blitzen center suggests displacement on boundary faults of about 4 km.

The Tuscarora district occupies the southeastern limb of the northeast-striking Mount Blitzen anticline through the middle of the Mount Blitzen center (Figs. 3 and 5). The anticline is largely restricted to the center but probably extends slightly northeast into the Big Cottonwood Canyon caldera. The anticline is mostly symmetrical, and dips average about 40°. However, the tuff of Mount Blitzen steepens to vertical along the southeastern limb near the margin of the volcanic center. Similarly, volcanoclastic sedimentary rocks and tuff (Tps) of the Pleasant Valley complex in the district just outside the center dip southeastward as steeply as 63°. The dips in the sedimentary rocks generally decrease to about 25° less than 1 km southeastward across the district.

The Mount Blitzen anticline has been interpreted to be an elongate dome resulting from emplacement of a large intrusion that parallels and underlies the anticline (Henry and Boden, 1998a). A prominent aeromagnetic anomaly that extends northeastward from the Mount Neva granodiorite into the middle of the Mount Blitzen center indicates that the anticline is underlain by an intrusion (Hildenbrand and Kucks, 1988; Henry and Ressel, 2000). The anticline is therefore analogous to resurgent domes in typical calderas. Late dikes of the Mount Neva intrusive episode are probably apophyses from this intrusion. The distinct northeast orientation of the anticline, the dike swarm, and the Mount Neva granodiorite probably reflects regional, northwest-oriented extension that affected the region in the Eocene (Clark et al., 1985; Seedorff, 1991; Snoke et al., 1997; Henry et al., 2001).

An alternative, purely tectonic origin for the anticline, involving tilting between two oppositely dipping, listric normal faults, is precluded by the anticline's timing and geometry. If tilting resulted from motion on the western and eastern boundary faults of the Mount Blitzen center, then basin formation, filling, and tilting would have occurred within about 100,000 years, an improbably short time for all these events to occur tectonically. Also, the tuff of Mount Blitzen should show progressive shallowing of dips upsection (i.e., fanning dips) if extension were contemporaneous with tuff deposition, but it does not. If, as we favor, tilting was later and affected the tuff of Big Cottonwood Canyon, tilting can not be related to the boundary faults, which are truncated by the tuff, or by any other known faults.

Northwest-striking faults cut the boundary faults of the Mount Blitzen center in and around the Tuscarora district and also host many of the veins (Figs. 3 and 5). Sense of displacement on these faults in the district is uncertain; rakes of striae on fault surfaces range from horizontal to vertical. Parallel faults farther southwest along the Mount Blitzen margin have definite strike-slip displacement, which suggests that those in the district do also. The northwest-striking faults may have formed during subsidence and segment the Mount Blitzen boundary faults. However, most of their displacement must have occurred during doming, because they cut the postsubsidence early porphyritic dacite (Tmd), and late dikes of porphyritic dacite (Tmdp) intrude along these faults to the southwest (Fig. 5).

Local Setting of the Tuscarora District

The Tuscarora district lies along and just outside the southeastern margin of the Mount Blitzen volcanic center (Figs. 3 and 5), and, on the basis of $^{40}\text{Ar}/^{39}\text{Ar}$ ages, ore formation was closely connected to the intrusions and structures of that center. The host rocks for ore are dominantly volcanoclastic sedimentary rocks and tuff (Tps) of the Pleasant Valley complex and early porphyritic dacite (Tmd) of the Mount Neva intrusive episode. The sedimentary rocks are undated in the district, but mapped relationships indicate that they are distal, reworked equivalents of the 39.9 to 39.7 Ma Pleasant Valley lavas to the southwest (Henry et al., 1999). The early dacite consists of numerous thick dikes, sills, and irregularly shaped intrusions in the sedimentary rocks. Hornblende from weakly propylitized dacite in the district has a $^{40}\text{Ar}/^{39}\text{Ar}$ age of 39.43 ± 0.13 Ma (Fig. 4 and Table 2). Several late dikes of the Mount Neva intrusive episode (Tmr and Tmdp) cut these rocks and the tuff of Mount Blitzen (Tbt) along the northwestern edge of the district. Although they do not host ore, the dikes commonly are propylitically altered and have quartz-adularia-pyrite selvages, indicating that they predate mineralization.

Tuscarora Ore Deposits

It has long been recognized that the Tuscarora district contains two deposit types of uncertain genetic relationship (Emmons, 1910; Nolan, 1936; Tables 3 and 4). A silver zone lies to the north and is characterized by relatively high Ag/Au ratios (Fig. 6), narrow alteration zones, and quartz-carbonate veins, commonly in early porphyritic dacite (Tmd). A gold zone lies to the south and is typified by relatively low Ag/Au ratios, more widespread alteration (Fig. 7), quartz-fissure veins, and areas of stockwork veining, commonly in tuffaceous sedimentary rocks (Tps). Although other differences are recognized (see below), Ag/Au ratio is the most distinctive difference between the zones (Table 4).

Exposures of mineralized rock in many parts of the district are poor, and workings, particularly those of the silver zone, are caved and inaccessible. Therefore, many of our samples are from mine dumps; it is not certain that the sampled rock is representative of ore, and the depth and plan location of the samples are unknown. In some cases, such as at the productive Grand Prize, Belle Isle, and Commonwealth workings (Fig. 5), ore-bearing structures are not exposed, in which case we rely on published structural data.

Silver zone

The Tuscarora silver zone is an area of about 1,200 by 1,500 m centered about 500 m northwest of Tuscarora. In addition to high Ag/Au ratios, deposits in this area are typified by multiple vein types including quartz + sulfide veins, carbonate + sulfide ± quartz veins, and late-stage comb quartz veins. In our samples, carbonate is all calcite, although scanning electron microscope-energy dispersive X-ray examination indicates minor iron, magnesium, and manganese in the calcite. Sulfides are mostly pyrite, but base metal- and Ag-bearing sulfides are common (Table 3). Iron and manganese oxide and hydroxide minerals are locally abundant, and early miners reported locally abundant Ag halide minerals.

TABLE 3. Structure, Host Rock, and Mineral Data for Mines and Deposits, Tuscarora Mining District

Mine, deposit	Vein system	Strike and dip of veins	Host rocks ¹	Ore minerals	Gangue minerals
Silver zone					
Navajo	Navajo	N 10°–25° W, 58°–80° W	Tps, Tmd	Ac, arj, asp, el (70/30), gal, prar, prou, sph	Qtz, ad, cc
Belle Isle	Navajo	N 10° W, W	Tps, Tmd		Qtz
North Belle Isle	Navajo	N-S, 35°–80° W	Tps	Gal, sph	Qtz, cc
Nevada Queen	Navajo	N 70° W, 80° N	Tps		Qtz, cc
Commonwealth	Navajo	Along N 50° W trend	Tmd	Clar, prar	Qtz, cc
N. Commonwealth	Navajo	Along N 50° W trend	Tps, Tmd	Gal, sph	Qtz, cc
Grand Prize	Grand Prize	Along N 75° E trend	Tmd	Ac, gal, prar, prou, sph	Qtz, ad, cc
Argenta	Grand Prize	N 60° E, 56° N	Tmd	Ac, prar	Qtz, ad, cc, mn
De Frees	Grand Prize	N 30° W, 55°–75° W; also N 80° E, 60° N	Tps, Tmd	Ac, agl, gal, sph	Qtz, mn
Independence	Grand Prize	NNW, W	Tps(?), Tmd(?)	Ac, agl, clar, gal, se, sph	Qtz, cc
Gold zone					
Dexter	Dexter	E-W, 15°–40° N stockwork zone; individual veins mostly NW, SW	Tps	Ac, arj, clar, el	Qtz, ad, mn
Young America	Dexter	N-S, 45°–60° W	Tps(?)	El (55/45)	
Eureka	Eureka	N-S vein system; individual veins N 15° W to N 10° E, 75°–88° W	Tps, Tpd	Asp, el (70/30)	Qtz, ad
Modoc	Modoc	N-S vein system; individual veins N 10° E, 45°–70° W	Tps, Tmd	Ac, cpy, gal, sph	Qtz, ad
South Modoc	Modoc	N 30° W to N 10° E, 80°–85° W	Tps		Qtz, ad
Battle Mountain	Battle Mountain	N 15° W, 80° W; also random stockwork veins	Tps, Tpl		Qtz

Mineral abbreviations: ac = acanthite, ad = adularia, agl = agularite, arj = argentojarosite, asp = arsenopyrite, cc = calcite, clar = chlorargyrite, cpy = chalcopyrite, el = electrum (atomic Ag/Au), gal = galena, mn = manganese oxides, prar = pyrrargyrite, prou = proustite, qtz = quartz, se = native selenium, sph = sphalerite

¹ See Figure 5 for unit name

TABLE 4. Characteristics of Tuscarora Epithermal Deposits and Carlin-Type Gold Deposits

Characteristic	Tuscarora (volcanic-hosted, epithermal) precious metal deposits		Carlin-type (sediment-hosted) gold deposits
	Silver zone	Gold zone	
Host rock	Eocene intrusive rocks > volcaniclastic rocks	Eocene volcaniclastic rocks > intrusive rocks	Mostly Paleozoic silty carbonates, but including Eocene dikes
Style	Narrow bonanza veins	Disseminated and stockwork veins	Highly variable; structurally to stratigraphically controlled; minimal veins
Alteration	Mostly narrow propylitic around veins	Mostly widespread silicification and adularization	Carbonate dissolution, argillization, and silicification
Age	39.3 Ma	39.3 Ma	Between ~42 and 36 Ma
Igneous association	With intrusions of 39.9 to 39.3 Ma Tuscarora volcanic field	Same as silver zone	Most with Eocene (40–36 Ma) igneous centers
Ore minerals	Pyrrargyrite, acanthite, electrum, galena, sphalerite, agularite	Electrum, acanthite	Submicron Au in arsenian pyrite
Common associated minerals	Calcite, pyrite, quartz, adularia, arsenopyrite	Quartz, pyrite, adularia, arsenopyrite, carbonate pseudomorphs	Quartz (as silicification of rock), calcite, orpiment, realgar, pyrite, arsenopyrite, stibnite, barite
Ag/Au	110 (this study) 150 (Nolan, 1936)	14 (this study) 4–5 (Nolan, 1936) 5.4 (Dexter pit)	0.05–2
Associated elements	As, Pb, Sb, Zn, Mn, Cd, Tl, Se, ± Hg, Mo	As, Hg, Sb, ± Mo, Tl	As, Sb, Hg, Tl, ± Ag, W, Te, Se, Ba
Pb isotopes	Pb sources are igneous rocks ± Paleozoic sedimentary rocks	Pb sources are igneous rocks ± Paleozoic sedimentary rocks	Pb sources are Paleozoic eugeoclinal rocks + igneous rocks
Measured $\delta^{34}\text{S}$	4.8–9.0	6.8–7.9	0–17, mostly 3–13
Fluid T (°C)	160–260	160–240	150–250
Salinity (wt % NaCl equiv)	1.6–2.2	1.2–1.6	<6
Fluid acidity	Probably near neutral	Probably near neutral	Slightly acidic
Depth	<1 km	<1 km	0–5 km; most ≥2 km(?)
Boiling	Present	Present	Not identified

Data from this study and Nolan (1936), Arehart (1996), Hedenquist and Lowenstern (1994), Hofstra (1994, 1997), Hofstra and Cline (2000), Phinisey et al. (1996), Ressel et al. (2000a, 2000b), and Tosdal et al. (1998)

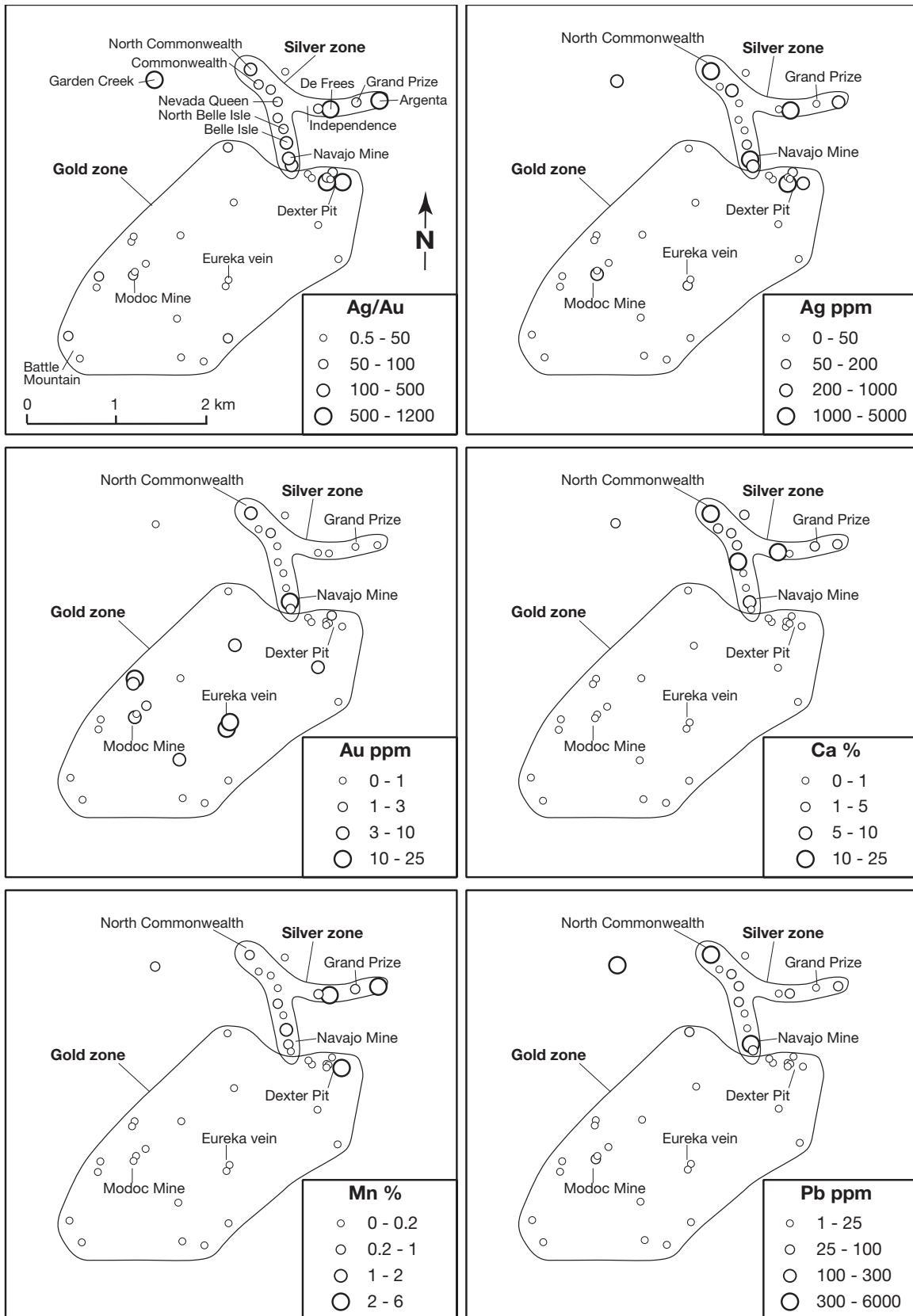


FIG. 6. Sketch maps depicting distribution of anomalous values of selected elements; values derived from assays of veins and altered wall rock from outcrop and mine dumps of the Tuscarora district. Data from Table 5. Where more than one value is available for a site, the highest value has been used.

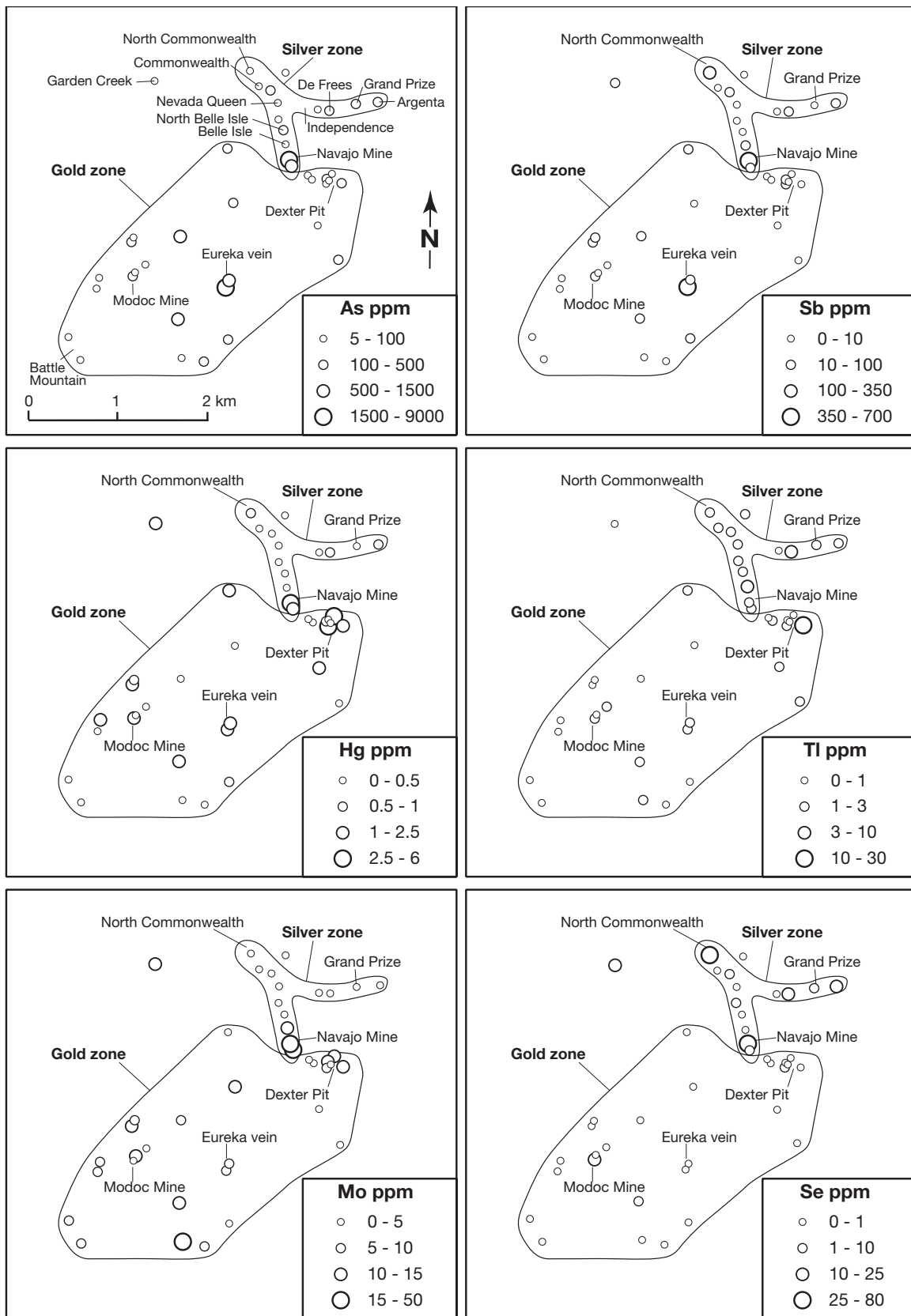


FIG. 6. (Cont.)

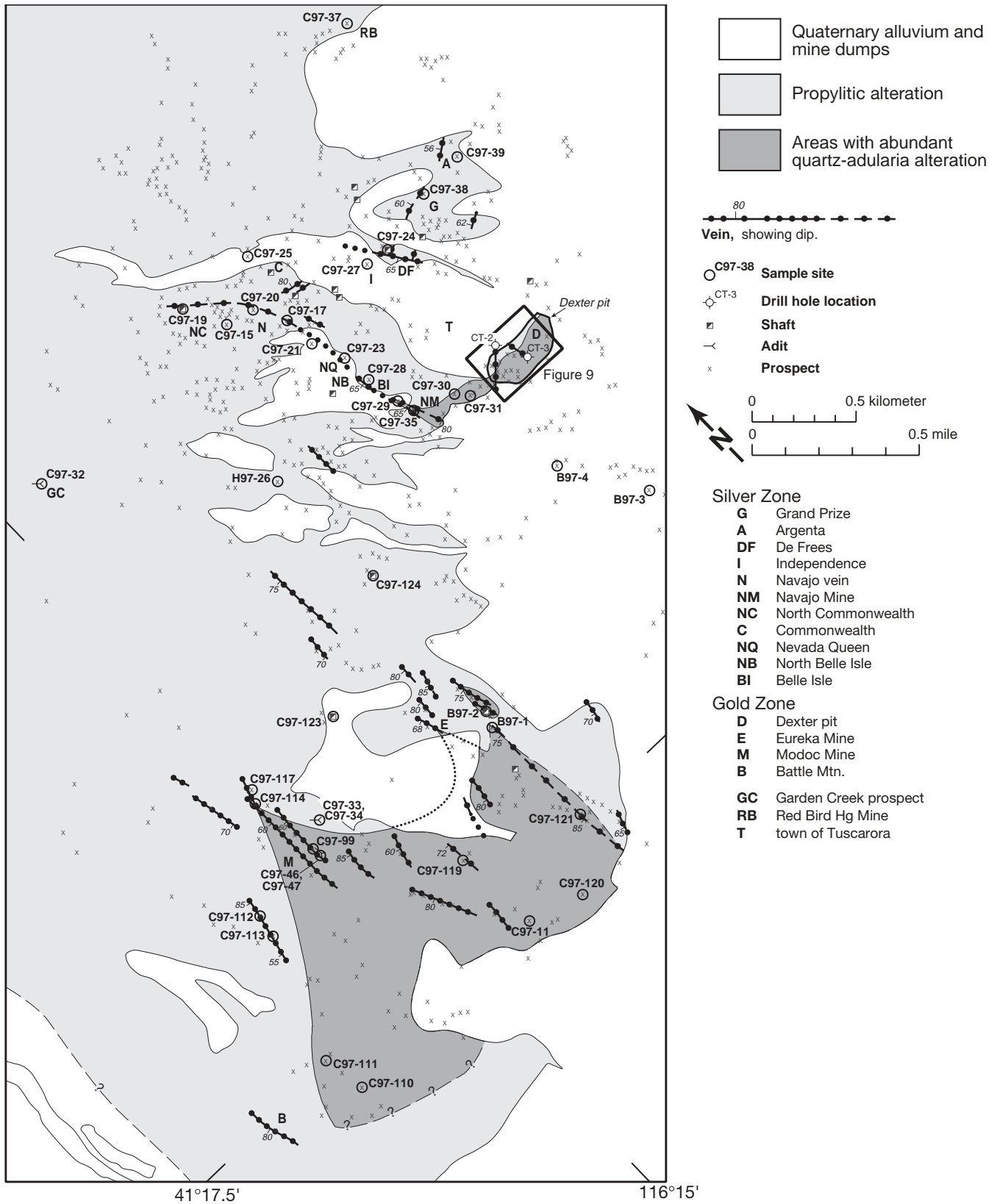


FIG. 7. Alteration and sample location map of the Tuscarora district; same area as in Figure 5. Note map is oriented north-east-southwest. Modified from Henry et al. (1999).

Navajo lode: The Navajo lode, a vein system that strikes north-northwest and dips west, was mostly exploited by the Navajo, Belle Isle, North Belle Isle, and Nevada Queen Mines (Table 3). Emmons (1910) included the Commonwealth and North Commonwealth Mines, which lie along a northwest-striking extension to the north (Fig. 5). The main Navajo shaft is caved and nearby outcrops mostly covered with mine waste. On the basis of dump materials, country rock at the shaft is mostly fine-grained tuffaceous sedimentary rock (Tps), although early porphyritic dacite (Tmd) is exposed nearby. This is also the case at the Belle Isle mine. Oxidized exposures of the Navajo lode, or subsidiary veins, are southwest and north of the Navajo shaft in surface stopes and prospects.

At the Navajo mine dump, blocks of Ag- and Au-rich, quartz-sulfide vein to 10 cm thick contain cubes and framboids of pyrite, along with late veinlets that contain pyrrargyrite, acanthite, and electrum (Fig. 8A). The pyrrargyrite has been partly replaced by intergrown acanthite and argentojarosite. Pyrrargyrite veinlets were also noted at the Commonwealth mine. Vein samples from other mines along the Navajo lode are mostly carbonate + sulfide minerals. Silver and base-metal sulfides with or without arsenopyrite occur in pyrite in some samples (Fig. 8B).

Grand Prize mine area: The Grand Prize mine area includes the Grand Prize, Argenta, De Frees, and Independence mines (Fig. 5). The Grand Prize mine had the largest recorded production in the Tuscarora silver zone from a sulfide-rich vein about 2 m wide (Nolan, 1936). According to Whitehill (1876), Nolan (1936), and Crawford (1992), the Grand Prize area mines exploited deposits along east-northeast-striking and northwest-dipping structures. However, Emmons (1910) reported that the Independence and Grand Prize veins approximately parallel the Navajo lode, and modern drilling indicates that the Independence vein strikes north-northwest (E. Struhsacker, pers. commun., 2001). Our mapping (Henry et al., 1999) showed that both east-northeast-striking and northwest-striking mineralized structures are present at the De Frees mine (Table 3). West-northwest-striking veins southeast of the Commonwealth mine may link the northwest-striking north segment of the Navajo lode with east-northeast-striking Grand Prize structures (Fig. 5).

Mineralized rock from the area includes silicified rock with sulfides as well as quartz ± adularia ± carbonate ± sulfide ± Mn oxide veins. Some comb quartz veins contain late pyrite and bladed calcite (Fig. 8C). Ore minerals include base-metal and silver-bearing sulfides (Table 3). Rich ore from the Grand Prize mine was reportedly “mostly sulphuret (*acanthite*) with a little ruby (*pyrrargyrite* and/or *proustite*) intermixed, and scarcely any quartz” (Whitehill, 1878, italicized words inserted by us).

Gold zone

Mines and prospects in the gold zone occur throughout an area of about 1,500 by 3,000 m from the town of Tuscarora southwest to Battle Mountain and possibly as far as Beard Hill and Castile Mountain (Figs. 3 and 5). Host rocks are tuffs, lavas, and intrusions of the Pleasant Valley volcanic complex (Tps, Tpb, and Tpd) and early porphyritic dacite

(Tmd). In addition to relatively low Ag/Au ratios, the ore is characterized by stockwork to sheeted or en echelon fissure veins of finely granular to comb quartz. Carbonate is not present, although we found quartz after bladed carbonate crystals at several sites. Sulfides, mainly pyrite, are common in unoxidized rock, and arsenopyrite is present in some samples. Base metal sulfides are rare (Table 3). Mn minerals are rare in gold zone ore, except in the Dexter pit.

Dexter mine: The Dexter mine was the most productive property in the gold zone (Crawford, 1992). As first noted by Nolan (1936), Ag and Au mineralization in the Dexter mine area is associated with widespread silicification and adularization in bedded rocks (Tps). Earlier workers described these rocks as “rhyolite” (e.g., Emmons, 1910). However, most of the ore in the Dexter open pit was in altered lapilli-fall or pumice-flow tuffs and fine-grained tuffaceous sedimentary rocks, which dip moderately to steeply southeast (Fig. 9). Crosscutting early porphyritic dacite (Tmd) occurs beneath the Dexter open pit and along the north wall of the pit. In the latter area a large mass of this dacite overlies the tuffaceous rocks along an east-striking contact that dips shallowly to moderately northward (Fig. 9). The overlying dacite is cut locally by shear zones with adularia-silica alteration; however, the dacite is mostly propylitized and typically not an ore host. Emmons (1910) described the Dexter deposit as a strongly fractured, north-dipping, 400 × 60 m zone with pockets of rich ore; he proposed that the entire mass was suitable for bulk mining at the time. Emmons further noted that the deposit contained numerous randomly oriented veinlets, in some cases containing adularia, and was locally rich in Au. Veins that we observed in the Dexter pit include randomly oriented limonitic comb quartz ± adularia ± pyrite, quartz-cemented breccia with pyrite, and quartz-free veinlets of limonite, hematite, and Mn oxide. Ore minerals at the Dexter pit are electrum, acanthite, and secondary minerals (Table 3). Pyrite is replaced or rimmed by acanthite ± argentojarosite with interlayered textures that indicate alternating sulfide and oxide deposition during supergene Ag enrichment (Fig. 8D).

The Young America mine, just north of the Dexter pit and directly under the town of Tuscarora, was reported by Whitehill (1876) to be on a north-striking, west-dipping, 1-m-wide vein. Unpublished maps (Crawford, 1992; Chevron Resources Company, 1989; Tuscarora Project, item 49500045, Nevada Bureau of Mines and Geology Information Office, Reno, Nevada) show a vein in this location that extends nearly 1,000 m to the Independence mine in the silver zone.

Modoc and Eureka veins: The Modoc and Eureka vein systems are north-trending zones of west-dipping, en echelon veins (Fig. 7 and Table 3). They include single veins, sheeted to braided veins, and breccia zones. On the basis of blocks on the Modoc mine dump, individual veins are as much as 30 cm thick and contain clasts of early vein material with base-metal sulfides and acanthite in late sulfide-poor granular to comb quartz. The acanthite may be of supergene origin on the basis of its occurrence as rims on corroded sphalerite (Fig. 8E). Quartz that replaced bladed calcite is common in specimens from the southern Modoc vein system. Gold ore from the northern part of the Modoc system contains chalcopyrite and malachite, the only copper minerals that we found in the main part of the Tuscarora district. Similar to the Modoc

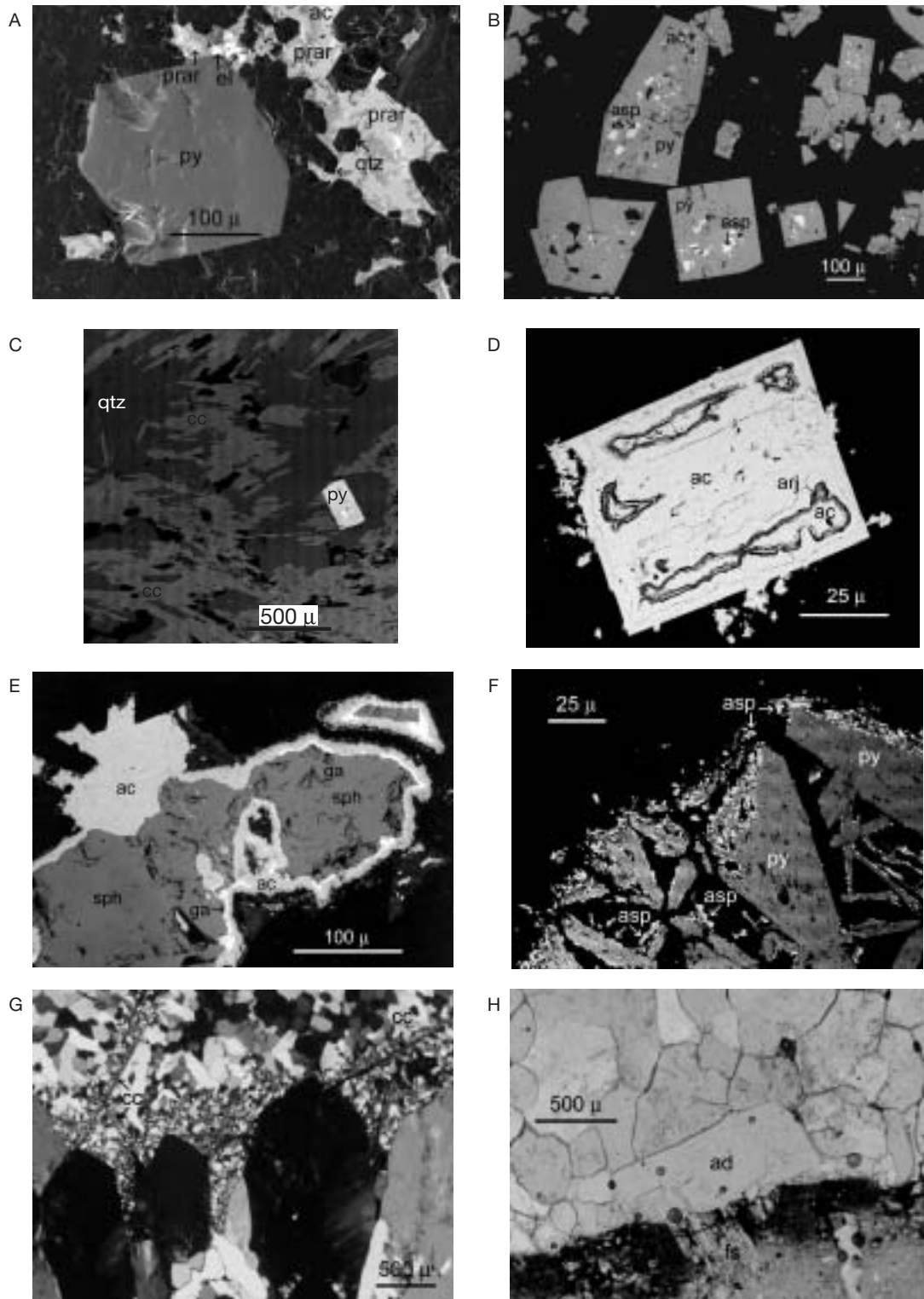


FIG. 8. Back-scattered scanning electron microscope images and photomicrographs. A. Late quartz (qtz), pyrrargyrite (prar), acanthite (ac), and electrum (el) veinlet on pyrite (Navajo mine dump; C97-29E). B. Pyrite cubes (py) with inclusions of arsenopyrite (asp) and acanthite (tiny, bright) (workings south of Navajo shaft; C97-35C). C. Late bladed carbonate (cc) and pyrite (py) in granular quartz (qtz) (Grand Prize mine; T32GP). D. Pyrite euhedron replaced by acanthite (ac) with irregular internal cavities filled with finely banded argentojarosite (arj) and acanthite (Dexter pit; C97-90A). E. Sphalerite (sph) rimmed by galena (ga), which is in turn rimmed by acanthite (ac) (Modoc mine dump; C97-47). F. Pyrite (py) in unusual tabular grains possibly after marcasite overgrown with arsenopyrite (asp) (Eureka vein; B97-1). G. Comb quartz vein with late bladed carbonate (cc) replaced by quartz, limonite, and clay (Dexter pit; T36DP). H. Vein composed mainly of comb quartz with minor adularia (ad) rhombs along vein walls adjacent to altered feldspar (fs) (Dexter pit; T36DP).

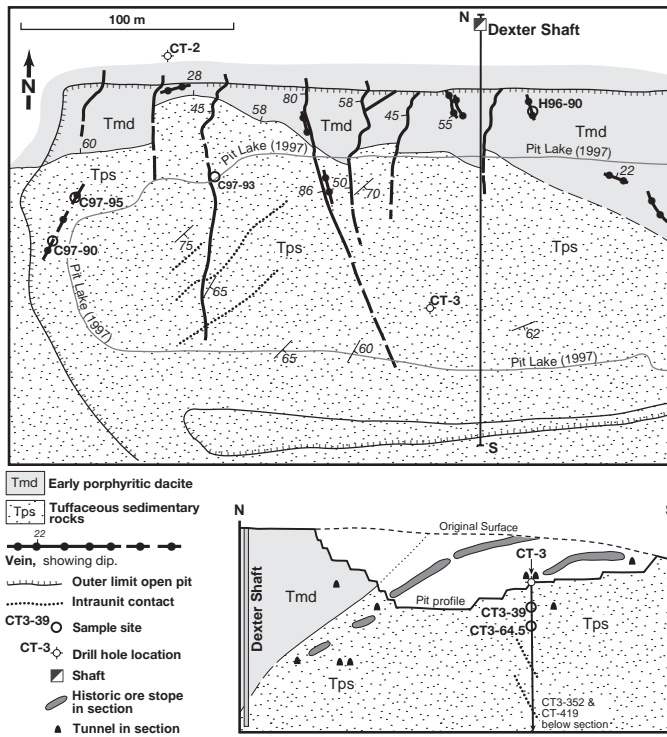


FIG. 9. Geologic map and cross section of the Dexter mine. Lithologic and structural symbols as in Figure 5. In part from 1:240 map by S.G. Zahoney, 1998, and 1:240 cross section by A.C. Milner, 1935, items 49500096 and 49500063, Nevada Bureau of Mines and Geology Information Office, Reno, Nevada.

veins, samples from the Eureka veins at Tuscarora contain sulfide-rich fragments set in sulfide-poor quartz; however, sulfides in the Eureka veins consist mostly of pyrite and arsenopyrite (Fig. 8F). We found electrum as irregular grains to nearly 0.5 mm across between late quartz crystals in Eureka vein ore.

Battle Mountain area: Workings on the east flank of Battle Mountain, 4 km southwest of Tuscarora, are in stockwork pyrite \pm quartz veins in adularized lavas (Tpl). This area was cited by Emmons (1910) and Nolan (1936) as having potential for low-grade disseminated Au mineralization (both writers referred to it as Beard Hill, a feature now shown on topographic maps about 2 km to the west). Drilling in the 1980s confirmed a small Au resource (E.M. Struhsacker, 1992, Tuscarora project, Elko County, Nevada, unpublished report for Corona Gold, 21 p.).

Other mineral prospects

Minor amounts of mercury were produced from cinnabar and metacinnabar veins in lavas of Sixmile Canyon at the Red Bird mine about 1 km northeast of the silver zone. Also, breccia containing galena, sphalerite, and chalcopyrite occurs at the small Garden Creek prospect within the Mount Blitzen volcanic center about 1 km west of the silver zone. Because of their settings and metal compositions (Table 5), neither occurrence may be related to precious-metal mineralization within the main district.

Alteration

At Tuscarora, alteration styles partly correlate with the two mineralized zones and partly with host rock (Nolan, 1936). The silver zone veins are commonly in propylitically altered (chlorite + calcite + albite + sericite + pyrite) early porphyritic dacite (Tmd), whereas alteration in the gold zone includes widespread silicification and adularization, typically in tuffaceous rock (Tps; see Fig. 7). Nolan (1936) ascribed these differences to the development of narrow fracture zones in the relatively massive and impermeable dacite and of wider, more diffuse shear zones in the more permeable tuffaceous rocks. In general, we found that dacite and other massive rocks throughout the district are propylitized, and more intensely altered rocks in both zones are converted to quartz + adularia \pm clay. Hypogene clays in both zones are kaolinite and montmorillonite.

Alteration in the Dexter pit and southern Navajo vein area (Figs. 5 and 7) illustrate the host rock control on alteration. Tuffaceous sedimentary rocks (Tps) in a 150 \times 800 m area are pervasively altered to quartz + adularia + clay, whereas early porphyritic dacite (Tmd) along the north pit wall and in drill core from beneath the pit (CT-3) is variably propylitized. At the Navajo mine, a narrow band of tuffaceous strata has been strongly altered to quartz + adularia + clay, but dacite only 30 m away is relatively unaltered. Nevertheless, distribution of the two types of alteration was not entirely dependent on host rock. Early porphyritic dacite (Tmd) and a dacite dome (Tpd) that host the Eureka and Modoc veins are pervasively silicified and adularized in places. Additionally, although early porphyritic dacite (Tmd) is the dominant rock type on many of the silver zone's dumps, tuffaceous sedimentary rocks (Tps) hosted ore at the Navajo, De Frees, and North Commonwealth mines. Therefore, the narrow vein deposits in the silver zone did not develop solely in massive, impermeable dacite.

The southwest part of the district shows evidence of regional variation in alteration. The northern Eureka vein system cuts propylitically altered Tmd with minor silica-adularia alteration, but to the south the veins lie along the eastern edge of a wide zone of silicification and adularization that appears to merge westward with similar alteration in the Modoc mine area (Fig. 7). At the Modoc mine, veins are in a 400-m-wide zone of quartz-adularia alteration that narrows and splits into thin apophyses along individual veins and faults to the north. However, to the south this alteration zone widens and appears to merge southwestward with pervasive alteration associated with the stockwork veins on Battle Mountain.

Geochemistry of Mineralized Rocks

Compositions of mineralized samples from Tuscarora reveal obvious differences between the silver and gold zones but also some overlap in the area of the Dexter pit and south end of the Navajo vein (Tables 4 and 5; Fig. 6). Mineralized samples from the silver zone, in addition to higher concentrations of Ag and Ag/Au, have higher Ca, Pb, Mn, Zn, Cd, Tl, and Se also. The gold zone has higher concentrations of Au, Hg, and Mo. Both zones have relatively high As and Sb and low Bi, Te, and W (not reported in Table 5; all samples have 10 ppm or less). Cu concentrations, which are generally low

TABLE 5. Chemical Analyses of Veins and Altered Wall Rock from Outcrop and Mine Dumps, Tuscarora Mining District

Sample	Latitude	Longitude	Ag	Au(ppb)	Ag/Au	K (%)	Ca (%)	Mn (%)	Fe (%)	Cu	Zn	As	Se	Mo	Cd	Sb	Te	Ba	Hg	Tl	Pb	Bi
Gold zone																						
B97-1	41°18.06'	-116°14.28'	68.3	17,700	4	2.03	0.04	7	6.26	15	3	8,901	0.9	8.01	0.00	656	0.00	115	1.81	2.24	24.1	0.40
B97-2	41°18.10'	-116°14.26'	18.8	14,800	1	2.14	0.05	19	1.51	6	9	982	0.5	8.87	0.03	62.8	0.09	515	2.28	1.96	10.1	0.59
B97-3	41°18.22'	-116°13.36'	1.0	81	12	5.64	0.02	13	0.69	3	2	107	0.0	2.25	0.05	6.3	0.14	1,215	0.19	1.21	18.4	0.54
B97-3A	41°18.22'	-116°13.36'	1.5	122	12	4.36	0.07	34	0.72	6	3	58	0.1	1.16	0.05	8.8	0.09	1,395	0.40	1.54	7.6	0.46
B97-4	41°18.43'	-116°13.53'	11.5	7,420	2	0.33	0.02	10	0.44	7	3	22	0.0	1.72	0.05	4.8	0.20	211	1.19	1.16	1.8	0.48
C97-11	41°17.63'	-116°14.65'	0.3	16	17	5.92	0.06	23	0.68	3	5	35	0.1	1.83	0.02	4.6	0.07	1,242	0.10	0.70	5.0	0.45
C97-11A	41°17.63'	-116°14.65'	0.4	268	2	0.05	0.06	26	0.29	2	3	5	0.0	26.6	0.02	9.3	0.13	89	0.40	1.03	4.7	0.67
C97-30	41°18.74'	-116°13.61'	0.0	42	0	6.75	0.16	441	1.55	8	55	48	0.3	3.37	0.15	3.1	0.13	1,547	0.03	0.85	22.0	0.51
C97-31	41°18.72'	-116°13.57'	2.8	157	18	5.20	0.07	13	0.53	4	6	28	0.2	2.13	0.03	2.2	0.00	1,456	0.02	1.17	5.1	0.40
C97-33	41°18.21'	-116°14.94'	15.4	1,370	11	2.36	0.06	929	1.66	20	49	17	0.7	6.01	0.39	2.1	0.13	628	0.19	1.46	37.3	0.43
C97-34	41°18.21'	-116°14.94'	1.4	208	7	6.27	0.13	1,071	2.44	19	94	31	0.3	2.53	0.83	1.6	0.00	1,502	0.44	1.01	21.1	0.44
C97-46	41°18.14'	-116°15.04'	8.7	112	78	4.94	0.07	23	1.46	3	12	146	0.3	3.38	0.06	3.1	0.12	700	0.58	1.64	36.3	0.53
C97-47	41°18.14'	-116°15.04'	777	5,270	147	4.21	0.01	18	1.35	5	398	142	23.8	1.38	1.61	36.6	1.80	562	1.29	1.94	463	1.04
C97-90	41°18.69'	-116°13.46'	3,681	652	5,646	3.60	0.02	27	2.02	15	12	46	4.6	5.60	0.02	41.6	0.10	1,015	3.40	1.32	71.5	0.43
C97-93	41°18.72'	-116°13.43'	0.0	331	0	4.44	0.05	71	0.99	13	30	28	0.4	3.00	0.07	4.6	0.15	1,266	0.15	0.39	9.3	0.21
C97-95	41°18.73'	-116°13.45'	38.2	508	75	1.47	0.08	142	12.96	35	77	268	0.7	11.6	0.28	15.2	0.14	150	0.59	0.48	20.7	0.37
C97-99	41°18.16'	-116°15.02'	0.8	99	8	6.01	0.02	40	0.79	2	2	37	0.2	8.52	0.01	1.0	0.16	1,836	0.21	0.69	9.7	0.29
C97-110	41°17.77'	-116°15.57'	8.1	471	17	7.72	0.03	22	2.99	4	4	38	0.8	4.95	0.02	1.5	0.13	66	0.28	0.52	21.2	0.28
C97-111	41°17.77'	-116°15.57'	7.0	90	78	8.97	0.19	35	1.57	3	6	22	0.0	2.95	0.02	1.1	0.11	438	0.14	0.44	13.7	0.21
C97-112	41°18.13'	-116°15.31'	12.1	111	109	2.81	0.07	63	1.70	15	8	76	0.9	4.64	0.03	5.0	0.18	497	1.84	0.50	24.9	0.29
C97-113	41°18.06'	-116°15.34'	3.8	274	14	6.36	0.10	36	1.52	17	13	96	1.0	5.30	0.05	3.4	0.09	1,919	0.13	0.40	19.0	0.37
C97-114A	41°18.35'	-116°15.05'	2.8	3,440	1	3.44	0.09	235	2.21	8	30	124	0.0	7.66	0.09	34.7	0.16	759	1.18	0.62	19.6	0.33
C97-117	41°18.38'	-116°15.03'	25.3	16,900	1	1.35	0.08	294	1.13	276	17	37	0.2	6.04	0.08	10.5	0.33	284	0.76	0.59	45.5	0.30
C97-119	41°17.87'	-116°14.68'	15.1	3,310	5	2.65	0.05	32	2.96	11	12	1,195	3.3	9.08	0.03	15.4	0.17	236	2.39	1.51	20.8	0.26
C97-120	41°17.60'	-116°14.47'	1.8	127	14	6.86	0.13	46	1.42	3	21	111	0.2	4.94	0.05	2.4	0.15	1,876	0.00	0.44	10.0	0.33
C97-121A	41°17.74'	-116°14.27'	1.2	36	33	5.63	0.09	39	1.96	4	11	110	0.7	3.65	0.07	16.9	0.17	2,058	0.65	0.44	8.6	0.15
C97-123	41°18.38'	-116°14.65'	1.6	232	7	5.99	0.15	34	2.02	3	7	1,310	0.6	8.73	0.03	26.9	0.11	115	0.09	0.44	15.5	0.25
C97-124	41°18.58'	-116°14.21'	8.9	4,650	2	2.04	0.05	27	0.80	5	8	103	0.7	7.57	0.03	2.5	0.13	866	0.25	0.49	15.0	0.26
CT2-211	41°18.76'	-116°13.41'	60.7	2,280	27	4.73	0.04	48	1.42	24	39	65	0.1	12.5	0.30	9.5	0.17	1,516	3.95	0.37	27.0	0.45
CT3-39	41°18.70'	-116°13.33'	15.7	30	523	5.01	0.10	1,912	9.20	7	165	70	0.1	5.15	0.11	4.6	0.15	1,859	0.09	2.36	59.8	0.32
CT3-64.5	41°18.70'	-116°13.33'	379	64	5,922	5.03	0.10	24,824	1.32	40	218	28	0.0	25.4	1.04	5.4	0.14	15,931	1.29	29.6	3.7	0.57
CT3-352	41°18.70'	-116°13.33'	2.7	44	60	4.13	0.13	74	1.36	2	63	33	0.1	4.28	0.01	2.7	0.15	1,835	0.07	0.39	15.7	0.33
CT3-419	41°18.70'	-116°13.33'	7.1	61	116	3.57	0.18	78	1.72	7	113	251	0.3	8.45	0.18	8.8	0.15	117	0.43	0.60	40.5	0.50
Mean			157	2,460	393	4.30	0.08	930	2.17	18	45	441	1.3	6.64	0.18	30.8	0.18	1,388	0.81	1.83	34.2	0.41
Median			7.1	232	14	4.44	0.07	36	1.51	7	12	65	0.3	5.15	0.05	5.0	0.14	866	0.40	0.70	19.0	0.40
High			3,681	17,700	5,922	8.97	0.18	24,824	12.96	276	398	8,901	23.8	26.6	1.61	656	1.80	15,931	3.95	29.6	463	1.04
Low			0.0	30	0	0.05	0.02	7	0.29	2	2	5	0.0	1.16	0.00	1.0	0.00	66	0.00	0.37	1.8	0.15
Silver zone																						
C97-15	41°19.30'	-116°14.00'	0.2	3	66	3.64	2.38	692	3.98	9	90	30	0.0	1.75	0.21	0.8	0.21	1,603	0.04	2.06	16.0	0.69
C97-17	41°19.20'	-116°13.85'	30.7	461	67	5.15	4.36	1,004	1.68	3	180	95	0.7	3.61	0.63	8.3	0.14	1,055	0.29	1.47	160.0	0.74
C97-19	41°19.40'	-116°14.07'	1,449	6,790	213	1.03	24.71	7,787	2.48	27	2,183	58	28.9	1.33	7.95	253	0.37	262	0.70	1.55	2,654	0.59
C97-19A	41°19.40'	-116°14.07'	0.0	17	0	5.08	1.60	1,111	2.10	6	78	41	0.3	1.09	0.22	5.5	0.18	1,504	0.03	0.97	16.4	0.50
C97-19B	41°19.40'	-116°14.07'	108	769	140	5.70	2.42	1,364	2.70	23	440	46	2.5	3.54	1.47	10.0	0.28	488	0.29	1.63	316	0.60
C97-19C	41°19.40'	-116°14.07'	31.4	267	118	4.41	0.11	271	2.16	11	637	52	6.1	2.81	2.30	3.9	0.37	451	0.13	1.43	1,189	0.74
C97-20	41°19.28'	-116°13.90'	303	2,050	148	5.31	1.34	780	2.65	7	99	112	2.7	3.32	0.30	45.6	0.27	312	0.32	1.45	349	0.71
C97-21A	41°19.10'	-116°13.85'	14.6	129	113	5.00	0.45	590	1.87	22	108	65	0.5	3.83	0.35	3.9	0.21	1,014	0.16	1.66	54.6	0.54
C97-21B	41°19.10'	-116°13.85'	3.5	120	29	17.73	2.631	2.07	2.07	37	897	90	1.7	2.23	3.28	2.2	0.34	378	0.15	1.71	457	0.79
C97-23	41°19.03'	-116°13.80'	3.9	107	36	5.03	0.08	76	1.32	1	14	112	0.3	3.75	0.06	3.0	0.25	802	0.26	1.61	27.4	0.65
C97-24	41°19.15'	-116°13.42'	69.2	627	110	6.80	0.13	28,924	3.55	35	1,248	335	8.7	20.0	1.29	6.2	0.66	811	0.50	2.26	478	0.99
C97-24A	41°19.15'	-116°13.42'	4,854	541	8,972	7.17	0.10	163	3.58	26	152	218	12.6	6.12	1.59	27.9	0.35	2,019	0.79	3.76	458	0.77

TABLE 5. (Cont.)

Sample	Latitude	Longitude	Ag	Au (ppb)	Ag/Au	K (%)	Ca (%)	Mn (%)	Fe (%)	Cu	Zn	As	Se	Mo	Cd	Sb	Te	Ba	Hg	Tl	Pb	Bi	
C97-24B	41°19.15'	-116°13.42'	78.1	151	517	4.52	0.05	76	0.67	2	6	62	0.3	3.24	0.05	3.4	0.22	1,285	0.18	1.95	40.3	0.68	
C97-25	41°19.39'	-116°13.79'	0.0	4	0	3.32	2.86	666	3.21	6	80	14	0.0	2.01	0.19	0.7	0.19	1,417	0.14	1.47	21.0	0.67	
C97-25A	41°19.39'	-116°13.79'	0.0	35	0	4.42	0.72	641	2.09	2	63	51	0.2	1.74	0.18	0.8	0.18	494	0.18	1.29	21.2	0.59	
C97-27	41°19.16'	-116°13.52'	10.7	119	90	5.14	0.08	193	1.93	4	52	94	0.4	5.45	0.10	5.3	0.08	1,177	0.17	0.95	33.1	0.46	
C97-27A	41°19.16'	-116°13.52'	9.4	112	84	3.06	12.94	6,331	3.31	4	72	59	0.0	2.13	0.20	2.7	0.00	833	0.03	0.87	21.8	0.35	
C97-28	41°8.94'	-116°13.78'	127	124	1,024	3.98	0.32	19,235	13.87	23	1,413	77	0.2	20.2	5.69	21.4	0.21	1,940	0.12	5.69	77.5	0.55	
C97-29	41°8.85'	-116°13.76'	684	2,380	287	4.65	8.01	2,948	7.02	26	5,699	241	10.5	1.36	18.10	68.0	0.00	109	2.09	0.97	1,765	0.89	
C97-29A	41°8.85'	-116°13.76'	2.7	86	32	2.23	0.04	114	2.73	3	11	149	0.6	26.6	0.03	6.5	0.03	454	0.03	0.99	69.2	0.75	
C97-29C	41°8.85'	-116°13.76'	1,671	1,970	848	2.65	0.06	103	6.13	32	209	1,515	7.7	23.7	0.60	32.3	0.14	111	0.10	1.73	911	0.61	
C97-29D	41°8.85'	-116°13.76'	324	816	397	2.41	0.05	135	11.03	11	243	771	7.3	7.64	0.36	64.9	0.14	104	5.03	1.77	596	0.43	
C97-29E	41°8.85'	-116°13.74'	4,808	24,700	195	2.80	0.06	263	13.18	39	279	303	77.9	8.43	0.87	355	0.28	49	1.10	2.68	3,745	0.34	
C97-35	41°8.81'	-116°13.74'	73.7	1,340	55	0.28	0.28	301	15.48	42	50	519	1.6	28.6	0.21	63.3	0.15	321	2.34	2.18	49.8	0.68	
C97-35A	41°8.81'	-116°13.74'	132	1,040	127	0.53	0.15	196	7.18	14	8	452	2.2	56.6	0.08	21.0	0.17	346	0.26	1.16	123	1.23	
C97-35B	41°8.81'	-116°13.74'	32.1	2,060	16	0.15	0.06	202	19.15	22	69	397	1.1	37.5	0.03	17.9	0.15	89	0.34	1.26	170	0.98	
C97-35C	41°8.81'	-116°13.74'	321	341	941	2.01	0.08	173	13.63	8	15	1,064	4.3	4.91	0.08	18.4	0.20	89	0.17	1.13	87.6	0.64	
C97-38	41°19.19'	-116°13.21'	22.0	178	124	4.13	0.11	46	1.91	8	24	108	3.2	3.19	0.08	6.2	0.16	504	0.14	1.02	43.8	0.59	
C97-38A	41°19.19'	-116°13.21'	9.2	242	38	3.40	2.99	3,274	2.07	24	53	237	0.9	1.59	0.14	6.6	0.22	310	0.02	1.02	31.1	0.38	
C97-38B	41°19.19'	-116°13.21'	4.4	347	13	6.19	0.15	32	2.39	7	16	497	3.1	4.45	0.15	7.4	0.16	222	0.40	1.35	28.3	0.47	
C97-39	41°19.20'	-116°13.03'	861	417	2,065	1.54	1.12	56,482	3.07	92	329	27	10.5	1.08	1.10	95.9	0.10	753	0.61	1.65	183	0.39	
C97-39B	41°19.20'	-116°13.03'	3.1	78	40	9.21	0.08	42	1.52	1	4	104	0.6	1.26	0.02	1.7	0.01	569	0.43	1.40	16.3	0.48	
H97-26	41°8.92'	-116°14.26'	9.8	410	24	3.15	0.09	186	2.94	54	93	142	0.1	2.56	0.20	12.3	0.17	1,049	1.61	1.55	130	0.55	
Mean			486	1,480	513	3.81	2.60	4,152	4.99	19	452	247	6.0	9.02	1.46	35.8	0.20	695	0.58	1.69	435	0.64	
Median			31.4	341	110	3.98	0.15	301	2.73	11	90	108	1.6	3.54	0.21	7.4	0.18	494	0.26	1.47	87.6	0.61	
High			4,854	24,700	8,972	9.21	24.71	56,482	19.15	92	5,699	1,515	77.9	56.6	18.10	355	0.66	2,019	5.03	5.69	3,745	1.23	
Low			0.0	3	0	0.15	0.04	32	0.67	1	4	14	0.0	1.08	0.02	0.7	0.00	49	0.02	0.87	16.3	0.34	
Garden Creek prospect																							
C97-32	41°19.34'	-116°14.85'	264	35	7,543	2.89	1.60	0	3.95	5,697	21,012	5	24.6	4.10	265	66.3	4.34	333	1.98	0.00	9,728	1.84	
Red Bird mine																							
C97-37	41°19.62'	-116°12.97'	0.0	0	0	2.73	2.14	0	3.22	16	127	9	0.0	1.70	0.09	5.0	0.10	1,473	20.9	0.96	5.0	0.43	

All analyses by ICP atomic-emission spectrometry, except Au by graphite furnace atomic absorption; complete analytical data in Henry et al. (1999)
 All data in parts per million except as noted

throughout the district, average slightly higher in the silver zone; however, the only high concentration (276 ppm) is in a sample from the Modoc vein in the gold zone.

Samples from the Navajo mine at the south end of the Navajo vein have high concentrations of Au, Hg, and Mo, more like those of the gold zone. A few samples from the Dexter pit have high concentrations of Ag, Mn, and Tl and high Ag/Au, although the high concentrations of Ag in Dexter pit samples result from supergene enrichment (acanthite and argentojarosite).

Ore Paragenesis

The important primary ore minerals in the Tuscarora district—electrum, pyrrargyrite, and acanthite—were deposited with quartz and adularia (Table 6). Ore and gangue minerals in the gold and silver zones followed roughly the same paragenetic sequence. However, ore mineralogy varies considerably from site to site, particularly in the gold zone. The quartz + adularia + precious-metal association is present in both the silver and gold zones, but pyrrargyrite was not identified in the gold zone. Supergene Ag enrichment was also important, and early bonanza Ag ore included rich accumulations of Ag halides. Secondary acanthite and argentojarosite were probably also important ore minerals.

Base-metal sulfides and some acanthite formed during an early vein stage in silver zone ore, as illustrated by inclusions of galena, sphalerite, acanthite, and arsenopyrite in pyrite (Fig 8B). A second precious-metal stage is represented by veinlets of pyrrargyrite, proustite, acanthite, electrum, quartz, adularia, and carbonate. A later stage of relatively barren carbonate veins and comb quartz veins locally cuts the sulfide-bearing ore, but these veins may be an extension of the second stage rather than a separate period of vein formation. Oxidation and supergene enrichment, represented by acanthite, chlorargyrite, argentojarosite, and native Se, along with Fe and Mn oxides, occurred during the third and final stage.

In the gold zone deposits, carbonate minerals are notably

absent, although textures indicate that bladed calcite has been replaced by quartz (Fig. 8G). Galena and sphalerite are minor constituents, except in samples from the Modoc mine, where sphalerite was deposited relatively early in quartz + adularia veins and predated galena and acanthite. At the Modoc and Eureka mines, fragments of early sulfide-rich vein material are set in late comb quartz. Similar to pyrite in the silver zone, early pyrite in the gold zone contains inclusions of galena and acanthite, and pyrite and arsenopyrite in the Eureka vein was also early and predated electrum. Electrum in gold zone deposits has compositions similar to electrum in silver zone deposits. We found electrum with late comb quartz at the Eureka mine, and earlier reports indicate that electrum occurs with adularia at the Dexter mine. Late acanthite in gold zone ore (Fig. 8D and E) may be wholly supergene.

Fluid Inclusion Microthermometry

A reconnaissance fluid inclusion study was performed on samples from the Navajo and Grand Prize mines in the silver zone and from the Dexter pit in the gold zone (Fig. 10). Inclusions were selected for measurement on the basis of textures indicating a primary origin or their occurrence in fluid inclusion assemblages with an established paragenesis (Goldstein and Reynolds, 1994). Ice melting temperatures were determined first for each sample; homogenization temperatures were collected in 10-degree increments during a single heating run on each chip. Phase changes that would indicate the presence of CO₂ were not observed, indicating that CO₂ is minor, and inclusions are interpreted assuming H₂O-NaCl fluid compositions. However, crushing experiments were not performed to detect low concentrations of CO₂.

Silver zone fluids

Samples from the Grand Prize mine for which fluid inclusion data are available are mostly composed of comb quartz averaging 2 mm in length and lesser adularia. The comb quartz possesses classic textures in which crystals are narrow

TABLE 6. General Paragenetic Sequence

Mineral	Silver zone			Gold zone		
	Early vein	Late vein	Supergene	Early vein	Late vein	Supergene
Pyrite	█					
Arsenopyrite	█					
Galena	█					
Sphalerite	█					
Chalcopyrite	█					
Aguilarite	█					
Carbonate		█			█	
Quartz	█	█		█	█	
Acanthite	█					█
Adularia	█					█
Electrum					█	
Pyrrargyrite		█				
Proustite		█				
Chlorargyrite						█
Argentojarosite						█
Goethite						█
Mn oxide						█
Selenium						█
Scorodite						█
Malachite						█

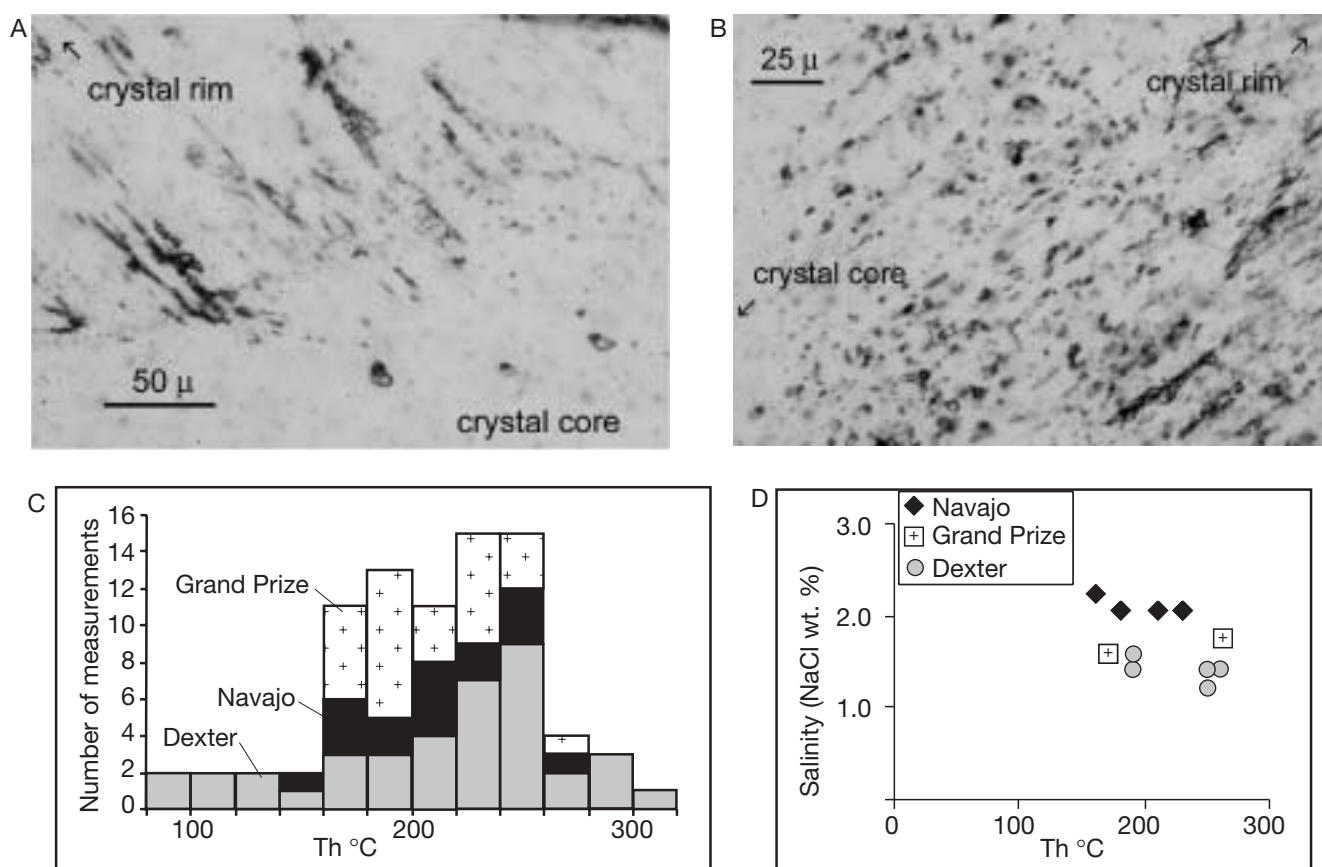


FIG. 10. A. Two-phase fluid inclusions (to $20\ \mu\text{m}$) with relatively smooth walls formed in the core of comb quartz crystals; tubular inclusions with irregular walls were trapped in crystallographically oriented arrays in crystal rims. Both populations of inclusions are primary (Grand Prize mine; T34GP1). B. Two-phase fluid inclusions to $15\ \mu\text{m}$ with relatively smooth walls close to quartz crystal core and stringy, irregular inclusions to $40\ \mu\text{m}$ long in the outer parts of the crystal; both are arranged in trains and are considered primary (Dexter pit; T36DP1). C. Plot of homogenization temperatures (T_h) measured on fluid inclusions from three samples from the Grand Prize mine, Navajo mine, and Dexter pit. Range of all temperatures is 80° to 320°C , but most are between 160°C and 260°C . D. Wt percent NaCl equiv salinities versus homogenization temperature for fluid inclusions.

Heating and freezing measurements were collected on a Linkam THMSG 600 heating and freezing stage attached to a CI 93 programmer and LNP cooling pump, and controlled by LinkSys software version 1.83. The stage was calibrated using synthetic fluid inclusions. Freezing measurements are accurate to $\pm 0.1^\circ\text{C}$ and homogenization measurements are accurate to within 2°C .

at the base, widen toward the center of the vein, and are terminated by crystal faces. Adularia occurs as small rhombs along vein walls and as grains as much as 5 mm wide that locally span vein widths. Other samples consist of breccia with quartz + adularia + carbonate + sulfide vein matrix. Adularia and sulfides (pyrite and minor sphalerite) occur near vein walls and are intergrown with the basal parts of comb to granular quartz that have an average grain size of about 0.5 mm. The interior of one vein consists of finely granular quartz with discontinuous masses of bladed carbonate and sparse pyrite cubes (Fig. 8C).

Two populations of primary two-phase fluid inclusions are present in much of the comb quartz. The cores of the wider parts of most crystals contain relatively equant, smooth-walled liquid plus vapor inclusions, approximately 5 to $40\ \mu\text{m}$ long (Fig. 10A). The inclusions are distributed throughout the crystal cores, and their restriction to the central parts of crystals indicates that they are probably primary; however, these

inclusions do not compose a single fluid inclusion assemblage because they were trapped as the interior of the crystal precipitated with time. Homogenization temperatures for these inclusions range from about 260° to 200°C . In general, higher-temperature inclusions are in innermost crystal cores, and lower-temperature inclusions surround the cores, reflecting declining fluid temperature with time. The second population of primary liquid plus vapor inclusions occurs in the outer rims of the quartz crystals. These inclusions are commonly long tubular, "stringy" inclusions that have irregular, rather than smooth, walls. The inclusions form crystallographically oriented arrays roughly perpendicular to crystal growth fronts (Fig. 10A). The crystallographic orientation and spatial distribution of these inclusions show that they are primary. Although many inclusion cavities grew during the same period of time, the inclusions did not all seal at the same time, and they do not compose a single fluid inclusion assemblage. Rather, the inclusions formed and sealed over time, and ho-

mogenization temperatures reflect changing fluid temperatures during this time. Many of these inclusions are necked; however, a region of inclusions with relatively consistent liquid/vapor ratios provided homogenization temperatures between 230° and 170°C (Fig. 10C). Freezing point depressions of -0.9° to -1.0°C from a small number of inclusions indicate low salinities for fluids trapped in the cores and rims of the quartz crystals (Fig. 10D). Secondary vapor-only and liquid-plus-vapor inclusions are present in anhedral quartz crystals that form irregular overgrowths on wall rocks and in comb quartz crystals in some veins; these inclusions record fluid boiling at this deposit.

The sample we examined from the Navajo mine is distinctly different from samples from the Grand Prize mine and does not contain comb quartz veins. The Navajo mine sample consists of pyrite-rich silicified country rock cut by veinlets composed of intergrown quartz, galena, and pyrrhotite, with traces of electrum and late acanthite and argentojarosite. The quartz forms equant to elongate grains that show crystal faces against the sulfide (Fig. 8A) and contains sparse secondary fluid inclusions. These inclusions generally have regular shapes and are less than 2 μm long, but a few reach 20 μm . Homogenization temperatures measured from three assemblages of secondary inclusions indicated minimum temperature ranges of 250° to 200°, 220° to 180°, and 180° to 160°C (Fig. 10C). The relative timing of these assemblages can not be determined, and these ranges indicate only that fluid temperatures varied at this location. Freezing point depressions are somewhat greater than those measured for the Dexter and Grand Prize samples and indicate salinities of 2.1 to 2.2 wt percent NaCl equiv (Bodnar and Vityk, 1994; Fig. 10D); alternatively the inclusions may contain minor amounts of CO_2 or H_2S .

Gold zone fluids

The sample from the Dexter pit contains two subparallel quartz + adularia veins each about 1 cm thick; one is composed of comb quartz crystals averaging 2 mm long with minor adularia rhombs along vein walls (Fig. 8H), and the other consists of similar comb quartz and traces of adularia, but it also contains limonite after early pyrite near vein walls and late bladed carbonate replaced by quartz, limonite, and clay (Fig. 8G). The comb quartz contains three populations of fluid inclusions and possesses some features similar to comb quartz from the Grand Prize mine. The first population consists of a small number of tiny, irregularly shaped fluid inclusions in narrow bases of the comb quartz crystals. On the basis of zoning in the quartz, they appear to be primary. A second population of larger (~2–15 μm), more regular and equant fluid inclusions formed in the cores of the wider parts of the crystals. The last population consists of tubular, irregularly shaped inclusions to 40 μm long that form crystallographically oriented arrays in the outer rims of the crystals, perpendicular to crystal growth fronts (Fig. 10B). At the transition from smooth-walled inclusions to tubular inclusions, both populations exist. The spatial distribution and textures of these three populations of inclusions indicate that they are primary. Homogenization temperatures measured on the equant fluid inclusions in the crystal cores indicate minimum fluid temperatures of approximately 200° to 260°C (Fig.

10C). Freezing point depressions of -0.8° to -0.7°C measured on a few inclusions indicate salinities of 1.2 to 1.4 wt percent NaCl equiv (Fig. 10D). Measurements were not made on the first and third primary populations owing to their small size and the lack of consistent liquid-vapor ratios in the inclusions. Textures suggest that both of these populations formed at temperatures of less than about 200°C (Bodnar et al., 1985).

Two populations of secondary inclusions were also identified in the comb quartz from the Dexter pit. One population consists of regularly shaped inclusions that are generally near the cores of the crystals. These inclusions provided a wide range in homogenization temperatures from 100° to 300°C, although most inclusions homogenized between about 190° and 260°C. The range in temperatures likely reflects, in part, trapping of inclusions at different times and inclusion leaking. A second population consists of vapor-only inclusions. These inclusions probably record fluid boiling that occurred sometime after deposition of the comb quartz.

Synthesis

Textures and fluid inclusion microthermometry indicate that quartz veins from mines in the gold and silver zones have similar thermal and paragenetic histories. Fluid temperatures cooled from between 260° and 230°C to less than 200°C, and fluid boiling occurred in both the silver and gold zone deposits. On the basis of the fluid inclusions, boiling was paragenetically late relative to the deposition of primary ore minerals in the silver zone but possibly coincident with deposition of ore minerals in the gold zone (e.g., late electrum in the Eureka vein). The presence of adularia that spans the time of mineralization suggests earlier boiling coincident with base-metal sulfide and silver deposition in the silver zone. Bladed carbonate is consistent with late boiling in both deposit types (Simmons and Christenson, 1994). Fluid inclusions at the Grand Prize mine and Dexter pit show that the cores of comb quartz crystals precipitated at temperatures as high as 260°C, although irregular inclusions in the earliest Dexter pit quartz suggest initial precipitation at less than about 200°C. After deposition from relatively high temperature fluids, the crystals continued to grow as fluid temperatures declined. The outer rims of quartz crystals precipitated at about 170°C, trapping parallel, crystallographically aligned arrays of tubular fluid inclusions. The total temperature drop indicated by these data approaches 100°C. On the basis of observations of geothermal systems, fluid temperatures may have declined in response to (1) incursions of cold water at the margins of systems, (2) waning of activity, (3) a falling water table, (4) recharge of cool surface waters in areas of high relief (Simmons, 1991; Hedenquist et al., 1992), or (5) energy consumption during boiling (Hedenquist et al., 1991; Simmons and Browne, 2000).

The paleodepth of Tuscarora mineralization is not tightly constrained. Boiling in the Dexter and Grand Prize deposits probably took place at temperatures of 200°C or less. At this temperature and low fluid salinity, the maximum depth of boiling below the water table would have been about 165 m. Boiling at depths of as much as 550 m might have been possible in earlier fluids with temperatures as high as 260°C (Haas, 1971).

Relationship between Ore and Structure

The precious-metal veins in the Tuscarora district are interpreted to occupy faults related to formation and doming of the Mount Blitzen center (Figs. 3 and 5). Three major sets of faults influenced vein orientations. A northeast-striking, moderately northwest-dipping set includes the fault that bounds the Mount Blitzen volcanic center and a fault that hosted the Grand Prize vein. The faults outboard of the Mount Blitzen boundary fault may have formed during initial subsidence of the Mount Blitzen center, but they may also have been reactivated during doming. Most of the major veins in the northern part of the district follow northwest-striking, steeply southwest-dipping faults. These veins also may have formed during subsidence but, as noted above, most of the displacement must have been during doming. The third set consists of faults and veins in the southern part of the district that dominantly strike north and dip steeply to the west. There may be a gradation between the northwest- and north-striking faults. For example, the major fault-controlled Navajo vein curves from a northwest strike near its northern end to a more northerly strike at its south end. Because Tuscarora district veins occur along these faults, which resulted mostly from doming, mineralization likely postdated most, if not all, tilting of the southeast-dipping host rocks.

Age of Mineralization

$^{40}\text{Ar}/^{39}\text{Ar}$ Ar dates on six samples of adularia, four from the gold zone and two from the silver zone, and on igneous rocks in and around the district, tightly constrain the time of mineralization to ~39.3 Ma. The adularia dates range narrowly between 39.32 ± 0.07 to 39.14 ± 0.07 Ma, and all but one fall between 39.32 and 39.24 Ma (Fig. 4). All six ages are indistinguishable within 2σ analytical uncertainties. The youngest adularia age is from Castile Mountain about 4 km southwest of the main part of the district (Fig. 3).

Dates on host rocks are only slightly older than the adularia dates. The date on weakly altered, early porphyritic dacite (Tmd) in the district constrains mineralization to be later than 39.43 ± 0.13 Ma. The late dikes in the district are undated, but dates on similar dikes to the north and west range from 39.51 ± 0.18 to 39.34 ± 0.04 Ma. The latter date is derived from sanidine from a dike about 6 km north of the district and is the most precise age for these dikes. If late dikes in the district are the same age, gold-silver mineralization likely occurred after 39.34 ± 0.04 Ma. The lavas of Sixmile Canyon (Tsd) are altered and host the Red Bird Hg mine. However, uncertainty in the relationship of the Hg mineralization to main Tuscarora mineralization means that the date of 39.25 ± 0.16 Ma on a Sixmile lava could be either premineralization or postmineralization. On the basis of analytic uncertainties, mineralization could have taken as much as about 300,000 years but could also have taken much less.

Lead Isotopes

Seven samples of feldspars from Tuscarora igneous rocks, 10 samples of sulfides, and two adularia samples were analyzed for their Pb isotope compositions (Table 7). The sulfides are pyrite and one galena, but petrographic examination indicates that three pyrite samples had galena inclusions and one

had acanthite. Because the feldspars, such as adularia, and sulfides contain variable but relatively high concentrations of Pb and almost no U, their Pb isotope ratios have changed little through time and reflect the isotopic composition of the Pb source.

Except for two samples of 35 Ma rhyolites, feldspars in Tuscarora igneous rocks have a narrow range of $^{207}\text{Pb}/^{204}\text{Pb}$ and $^{208}\text{Pb}/^{204}\text{Pb}$ but somewhat more variation in $^{206}\text{Pb}/^{204}\text{Pb}$ (Fig. 11). The latter ratios form two clusters of three and two samples with differences that exceed analytical uncertainty. Two samples of the Mount Neva granodiorite fall into different clusters. The variation within the 39 Ma samples can be interpreted to indicate a contribution from Paleozoic sedimentary rocks in the higher $^{206}\text{Pb}/^{204}\text{Pb}$ group, but the fact that only five samples were analyzed limits interpretation. Tuscarora igneous rocks are less radiogenic than coeval Eocene igneous rocks from the Carlin trend. The 35 Ma rhyolites have much lower $^{206}\text{Pb}/^{204}\text{Pb}$ and higher $^{208}\text{Pb}/^{204}\text{Pb}$, which suggests a contribution from Archean crust.

All hydrothermal minerals except galena show narrow ranges of all ratios. Most hydrothermal minerals have isotopic ratios similar to those of the higher $^{206}\text{Pb}/^{204}\text{Pb}$ igneous rock group. $^{207}\text{Pb}/^{204}\text{Pb}$ and $^{208}\text{Pb}/^{204}\text{Pb}$ ratios of hydrothermal minerals show a greater spread than do those of the igneous rocks, but the differences are small. The galena has a noticeably lower $^{206}\text{Pb}/^{204}\text{Pb}$ ratio than other hydrothermal minerals; it plots with ratios of the lower $^{206}\text{Pb}/^{204}\text{Pb}$ cluster of igneous rocks, and one pyrite sample has a higher $^{207}\text{Pb}/^{204}\text{Pb}$ ratio.

The Pb isotope data are consistent with all Pb in hydrothermal minerals having been derived from Eocene igneous rocks. A contribution from Paleozoic sedimentary rocks is possible but not required. The difference between the galena sample and the other minerals reflects their different locations within the district (Table 7 and Fig. 7). The galena sample is from a prospect in tuff of Mount Blitzen within the downdropped Mount Blitzen center where Paleozoic rocks are probably several kilometers deeper than in the main district.

Sulfur Isotopes

The sulfur isotope compositions of vein sulfides from deposits in both the silver and gold zones were compared with those of bulk sulfur in fresh intrusions (Table 7) and with pyrite and barite in Ordovician rocks inferred to underlie the area. Mean $\delta^{34}\text{S}$ values for Ordovician pyrite and barite are from Hofstra (1994) from the Independence Mountains, about 15 km to the east.

Vein pyrites have $\delta^{34}\text{S}$ values between 4.8 and 9.0 per mil and galena has a value of 3.8 per mil. Pyrites from the Grand Prize and Queen mines, near the center of the silver zone, have the lowest $\delta^{34}\text{S}$ values, whereas pyrite from the North Commonwealth mine on the north end of the silver zone has the highest $\delta^{34}\text{S}$ value (Table 7). The other pyrite samples from both the gold and silver zones have nearly identical $\delta^{34}\text{S}$ values ($7.4 \pm 0.5\%$). Intrusive rocks have $\delta^{34}\text{S}$ values of 4.9 to 7.2 per mil and very low sulfur contents of 10 to 15 ppm.

The calculated $\delta^{34}\text{S}$ compositions of H_2S in equilibrium with pyrite and galena using fractionation factors in Ohmoto and Rye (1979) and a median temperature of 225°C range

TABLE 7. Pb and S Isotope Data, Tuscarora Mining District

Sample no.	Mineral	Vein or rock type	Mine	North latitude	West longitude	²⁰⁶ Pb/ ²⁰⁴ Pb	²⁰⁷ Pb/ ²⁰⁴ Pb	²⁰⁸ Pb/ ²⁰⁴ Pb	δ ³⁴ S (‰)	δ ³⁴ S (‰) ¹
Silver zone										
H96-104	Adularia	Navajo	North Commonwealth	41°19.4'	116°14.1'	19.067	15.676	39.080		
C97-19	Pyrite	Navajo	North Commonwealth	41°19.4'	116°14.1'	19.056	15.652	39.030	9.0	7.4
C97-20	Pyrite	Navajo	Nevada Queen	41° 9.3'	116°13.9'	19.072	15.676	39.083	4.8	3.2
C97-29E	Pyrite	Navajo	Navajo	41°18.9'	116°13.8'	19.105	15.706	39.196	7.7	6.1
C97-38B	Pyrite	Grand Prize	Grand Prize	41°19.2'	116°13.2'	19.076	15.649	38.991	5.5	3.9
C97-39B	Pyrite	Argenta	Argenta	41°19.2'	116°13.0'	19.078	15.651	38.997	6.9	5.3
Gold zone										
H96-98	Adularia	Dexter	West end Dexter pit	41°18.7'	116°13.6'	19.054	15.670	38.987		
C97-90	Pyrite	Dexter	Dexter pit	41°18.7'	116°13.4'	19.111	15.670	39.129	7.9	6.3
B97-1	Pyrite	Eureka	Unnamed	41°18.1'	116°14.3'	19.063	15.668	39.042	6.8	5.2
B97-2	Pyrite	Eureka	Unnamed	41°18.1'	116°14.3'	19.030	15.657	38.972	7.3	5.7
C97-47	Pyrite	Modoc	Modoc	41°18.2'	116°15.0'	19.006	15.662	39.034	7.6	6.0
Garden Creek prospect										
C97-32	Galena	Unnamed		41°19.4'	116°14.9'	18.891	15.673	39.097	3.8	6.3
Tuscarora igneous rocks										
H96-19	Sanidine	Rhyolite dike (Tmr)		41°22.4'	116°14.9'	18.835	15.661	39.034	5.6	
H96-72	K feldspar	Mount Neva Granodiorite (Tmg)		41°19.3'	116°21.6'	18.886	15.673	39.103	7.2	
NS2-9	K feldspar	Mount Neva Granodiorite (Tmg)		41.33°	116.33°	19.094	15.679	39.105		
H96-103	Plagioclase	Early porphyritic dacite (Tmd)		41°19.0'	116°13.6'	19.077	15.660	39.031	4.9	
H96-80	Sanidine	Tuff of Big Cottonwood Canyon (Tct)		41°24.5'	116°20.6'	18.872	15.663	39.103		
H96-59	Sanidine	Rhyolite lava (Twr; 35 Ma)		41°22.5'	116°19.4'	17.092	15.598	39.848		
DB-19	Sanidine	Rhyolite lava (Twr; 35 Ma)		41°19.3'	116°23.2'	17.833	15.625	39.268		

S analytical methods: compositions of vein pyrite and galena determined by an on-line method using an elemental analyzer coupled to a Micromass Optima mass spectrometer following Giesemann et al. (1994); analytical precision better than ±0.2 per mil; S extracted from igneous rocks from 20 gm aliquots using the Kiba reagent (Sasaki et al., 1979); the produced Ag₂S then used to perform sulfur isotope analyses using an Eurovector elemental analyzer interfaced with a Micromass IsoPrime stable isotope ratio mass spectrometer, also following the method of Giesemann et al. (1994); analytical uncertainty is ±0.3 per mil

Pb analytical methods: Wooden et al. (1998) and Tosdal et al (2000)

¹ Calculated composition of hydrothermal fluid in equilibrium with pyrite or galena at 225°C

from 3.2 to 7.4 per mil. The δ³⁴S_{H₂S} value for galena is similar to those for most of the pyrite samples consistent with both minerals having the same S source. The absence of hypogene sulfates in the veins suggests that ore fluids lacked appreciable sulfate (i.e., H₂S >> SO₄⁻²). Consequently, the calculated δ³⁴S_{H₂S} values represent bulk sulfur in the fluids. The δ³⁴S_{H₂S} values are indistinguishable from those in the intrusive rocks, suggesting that all of the H₂S could have been derived from a magmatic source either by leaching or directly from a magmatic fluid source. The δ³⁴S values from the intrusions are higher than typical magmatic δ³⁴S values of about 0 per mil in the western United States (Ohmoto and Rye, 1979), suggesting that the Tuscarora magmas may have obtained sulfur from country rocks. The Paleozoic sedimentary rocks inferred to underlie the veins and volcanic rocks are a likely source for sulfur with high δ³⁴S values. Assimilation of or exchange with Paleozoic rocks containing diagenetic pyrite (mean 12.6‰), organic sulfur (which typically has δ³⁴S values greater than those of diagenetic pyrite; Ohmoto and Rye, 1979), and barite (mean 27.4‰) can account for the high δ³⁴S values in the intrusions. Ore fluids did not have to circulate through underlying Paleozoic rocks to obtain their high δ³⁴S_{H₂S} values. However, any fluids that did circulate through Paleozoic rocks would also be expected to contain H₂S with high δ³⁴S

values. Thus, fluid circulation through Paleozoic rocks can not be excluded.

Discussion

Relationship of Tuscarora deposits to igneous activity and structures

Low-sulfidation epithermal deposits are commonly associated with intermediate to silicic magmatism (Heald et al., 1987; Lipman, 1992; White and Hedenquist, 1995; Henry et al., 1997; John, 2001), and the influence of igneous activity and structures on the Tuscarora deposits is particularly clear. Mineralization at Tuscarora formed along the southeast flank of the 39.8 to 39.7 Ma Mount Blitzen volcanic center, a caldera-like, fault-bounded basin filled with dacite domes and associated pyroclastic and volcanoclastic rocks. Precious-metal deposits in the district occur along and as much as 2 km outside the volcanic center. A system of northeast- and northwest-striking faults that parallel and are perpendicular to the margin largely controlled the distribution of veins and more disseminated deposits. The faults mostly resulted from doming of the Mount Blitzen center during the later Mount Neva intrusive episode.

The temporal association of mineralization and magmatism is even more straightforward. ⁴⁰Ar/³⁹Ar ages of adularia

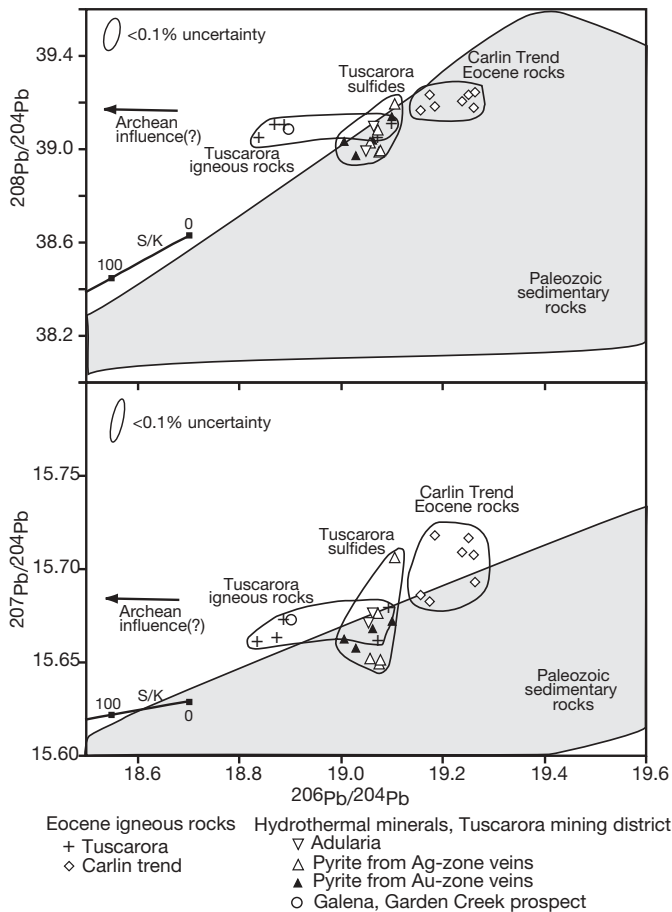


FIG. 11. Pb isotope compositions of Eocene igneous rocks and hydrothermal minerals of the Tuscarora mining district. Pb in the hydrothermal minerals may be derived entirely from igneous sources or may have a component of Paleozoic sedimentary rocks. Fields for Paleozoic rocks and for Eocene igneous rocks of the Carlin trend from Tosdal et al. (2000). S/K = Stacey-Kramers growth curve from 0 to 100 Ma.

cluster tightly at about 39.3 Ma. Host rocks are dated as young as 39.43 ± 0.13 Ma in the district and 39.34 ± 0.04 Ma outside the district (early porphyritic dacite, Tmd, and late rhyolite dike, Tmr, of the Mount Neva intrusive episode, respectively). These ages are consistent with late intrusions of the multiphase (39.5–39.3 Ma) Mount Neva intrusive episode being the heat source for hydrothermal activity and possibly a source of some ore components. The specific heat source could be either the large intrusion that we interpret to underlie the Mount Blitzen center and northeast-striking anticline or a smaller intrusion more directly beneath the Tuscarora district.

Note that mineralization at Tuscarora formed only when intrusive activity became dominant in the Tuscarora volcanic field. No mineralization is known to be contemporaneous with any of the preceding volcanic episodes, despite the considerable volume of magma and therefore heat that they represent.

Pb and S isotope data indicate that metals in the deposits were probably derived from igneous rocks of the Tuscarora volcanic field with a possible contribution from surrounding

Paleozoic sedimentary rocks. The low dD value of fluid inclusion water (-134‰) in comb quartz from the Grand Prize mine (Hofstra et al., 1999) and the low salinity of fluid inclusions from both zones (Fig. 10D) suggest that ore fluids consisted mostly of meteoric water, as with most low-sulfidation deposits (White and Hedenquist, 1995).

Origin of two types of deposits at Tuscarora

The silver vein deposits at Tuscarora belong to a class of low-sulfidation epithermal deposits (type 1; John, 2001) characterized by high Ag/Au ratios (10–100), appreciable base metals ($\text{Cu} + \text{Pb} + \text{Zn} > 200$ ppm), and dilute to moderate-salinity fluids. Possible analogs are Tonopah (Ashley, 1991) and the Comstock lode (Vikre, 1989; Brake and Romberger, 2000) in Nevada; Creede, Colorado (Bethke, 1988); and Tayoltita, Mexico (Smith et al., 1982). In contrast, the gold zone deposits belong to another low-sulfidation class (type 2) characterized by low Ag/Au ratios (< 10), low base metal contents even at depth ($\text{Cu} + \text{Pb} + \text{Zn} < 200$ ppm), and consistently dilute fluids (≤ 2 wt % NaCl equiv). Analogs include Round Mountain (Sander and Einaudi, 1990), Sleeper (Nash et al., 1995), Rawhide (Black et al., 1991) Buckskin-National (Vikre, 1985), and Bullfrog in Nevada (Eng et al., 1996); Oatman, Arizona (DeWitt et al., 1991); and El Piñon, Chile (Robbins, 2000). John (2001) demonstrated that these two deposit types form in distinct magmatic-tectonic settings in the Great Basin—type 1 in subduction-related andesitic arcs and type 2 with extensionally derived bimodal suites. Therefore, juxtaposition of these two deposit types in a single district, during a single episode of magmatism, is problematic.

The origin of and genetic relationship between the type 1 Ag-rich deposits and the type 2 Ag-poor deposits at Tuscarora remain uncertain. Two alternatives are possible: the two types of mineralization formed concurrently as zoned or evolving parts of a single hydrothermal system, or the two types formed from separate, compositionally distinct hydrothermal events that were coeval or nearly so. The two deposit types occur in different but adjacent areas and have different physical characteristics and distinct geochemical signatures, but they have similar paragenetic sequences, fluid inclusions, and Pb and S isotope characteristics (Table 4). Geochemical characteristics overlap somewhat where the two zones meet at the south end of the Navajo vein and in the Dexter pit, but the overlap is not obviously gradational. Although the deposits in the two zones have indistinguishable adularia $^{40}\text{Ar}/^{39}\text{Ar}$ ages, our dating can not distinguish temporally close events.

Single system: The crystallization sequence in quartz veins of the Dexter and Grand Prize deposits is similar: early adularia and quartz with sparse, primary fluid inclusions trapped at a high temperature; later, irregular fluid inclusions trapped at lower temperature; and, finally, bladed carbonate that indicates boiling (Fig. 10; Table 6). Fluid inclusion data show that quartz veins in the two zones have similar homogenization temperatures and salinities (Fig. 10C and D). Pb and S isotope data indicate that fluids in both zones had similar compositions and interacted with similar rocks. However, replacement of calcite in gold zone veins suggests late circulation of fluids that did not occur in silver zone veins.

A possible scenario for a single zoned or evolving hydrothermal system at Tuscarora is that the silver zone veins

were feeders to the more disseminated gold zone. Modeling shows that processes such as pH decrease and H₂S removal can separate base and precious metals in boiling epithermal systems (Spycher and Reed, 1989; Reed, 1998), and such processes may have produced the paragenesis in the Tuscarora district during a single hydrothermal episode. Another single-system scenario is that the focus of hydrothermal activity could have shifted southward as the system evolved. Our data suggest that mineralization postdated tilting of the host rocks, in which case evolving hydrothermal fluids would have had to spread laterally into the gold zone, rather than ascending into it.

Two systems: In the Tuscarora district, two critical points suggest that the two types are not a single, compositionally zoned system. First, distinct differences are evident in Ag/Au ratios (Fig. 6), base metal concentrations, and mineralogy between the silver and gold zones. These same characteristics are relatively consistent throughout wide areas and depths within types 1 and 2 low-sulfidation deposits, and the two deposit types do not grade into each other. Second, fluid inclusion data, although limited to samples from the Dexter, Navajo, and Grand Prize mines, are not consistent with the silver zone being a hotter or deeper feeder to the gold zone. The samples have comparable homogenization temperatures and salinities, and depths indicated by possible boiling temperatures are equivalent.

If the silver and gold zones at Tuscarora are spatially juxtaposed but temporally separate hydrothermal events, then the duration of both events must have been sufficiently brief that they can not be resolved by high-precision ⁴⁰Ar/³⁹Ar dating. The analytical errors for the ⁴⁰Ar/³⁹Ar age data for the Tuscarora deposits are such that the two styles of mineralization had to have formed within about 300,000 years. Studies of modern geothermal systems in New Zealand indicate that 1 Moz Au can be transported and 0.1 Moz can be deposited within 1,000 years (Hedenquist and Henley, 1985; Seward, 1989). Moreover, numerical modeling studies (Cathles, 1981; Cathles et al., 1997) and recent high-precision ⁴⁰Ar/³⁹Ar dating of epithermal and porphyry mineral deposits (Henry et al., 1997; Marsh et al., 1997) indicate that igneous-supported hydrothermal systems may last from only a few tens of thousands to 100,000 years and still deposit significant quantities of metals. Indeed, ⁴⁰Ar/³⁹Ar data from the giant volcanic-hosted Au-Ag deposit at Round Mountain (16 Moz Au) indicate that this deposit formed in less than 100,000 years and probably less than 50,000 years (Henry et al., 1997).

Significance for Carlin-type gold deposits

The temporal and regional association of the Tuscarora Ag-Au epithermal deposits with Carlin-type gold deposits is significant for understanding the regional metallogeny of this part of the Great Basin. Tuscarora lies 35 km north of the northern end of the Carlin trend and about 20 km southwest of Carlin-type deposits in the Independence Mountains (Fig. 2). Carlin-type deposits in the Great Basin are largely restricted to the region that also underwent Eocene magmatism, and the deposits formed contemporaneously with the Tuscarora pulse of magmatism. These relations are best illustrated for the Carlin trend, which contains about 60

percent of the known gold in Carlin-type deposits in the Great Basin (Hofstra and Cline, 2000) and lies within and next to a 700 km², 40 to 36 Ma Eocene igneous center, the largest known in the region (Henry and Ressel, 2000; Ressel et al., 2000a, 2001). Mineralization in the Carlin trend is interpreted to have occurred, possibly episodically, between about 40 and 37 Ma (Emsbo et al., 1996; Leonardson and Rahn, 1996; Ressel et al., 2000a, b). Although the role of Eocene magmatism in Carlin systems is still debated (Sillitoe and Bonham, 1990; Seedorff, 1991; Thorman et al., 1995; Ilchik and Barton, 1997; Henry and Ressel, 2000; Hofstra and Cline, 2000), the close association of Carlin-type deposits with regional magmatism raises the questions of whether a genetic link exists between epithermal and Carlin-type deposits and whether Carlin-type deposits exist at or near Tuscarora.

The Tuscarora deposits are in some ways similar to and in some ways quite different from Carlin-type deposits (Table 4). Important similarities are their ages, low temperatures of ore deposition, low salinities of the ore fluid, associated elements in the deposits, and similar S isotope ratios. Carlin-type deposits are distinguished by the dominant host rock (although some Carlin-type deposits are in Eocene igneous rocks), high Au/Ag ratio, ore mineralogy (submicrometer-size Au in trace element-rich pyrite), little or no vein quartz or adularia, generally greater inferred depth of formation and lack of boiling, and apparently more acidic fluid.

In a similar comparison of Carlin-type deposits and Miocene epithermal deposits of the northern Nevada rift, John et al (1999) and John and Wallace (2000) pointed out that the fluids that generated epithermal deposits could arise from Carlin-type fluids by boiling and mixing with meteoric water and that this change could account for most of the differences between the deposit types. In their model, magma could have released an ore fluid that had relatively low salinity, had significant H₂S and moderate CO₂ and was therefore slightly acidic. Such a fluid could transport Au, the common trace elements of both Carlin-type and epithermal deposits, and low concentrations of base metals. This fluid could generate Carlin-type deposits along with their characteristic alteration (carbonate dissolution, argillization, and silicification) at depth. At shallower depths, release of CO₂ and H₂S during boiling and mixing with meteoric water would raise fluid pH to approximately neutral, causing Au and Ag deposition. The evidence for boiling in epithermal deposits and the lack of boiling in Carlin-type deposits is consistent with this model.

If epithermal fluids are evolved versions of Carlin-type fluids, then Carlin-type deposits could lie beneath Tuscarora. Upper-plate Paleozoic rocks underlie the district, probably at depths of 500 to 1,000 m. The more favorable lower-plate rocks lie at greater depths but probably less than the maximum 5 km depth of inferred formation of Carlin-type ore (Hofstra and Cline, 2000). Henry and Ressel (2000) suggested that Carlin-type deposits are associated with Eocene magmatism and favored by igneous centers that were dominated by intrusions. If true, Carlin-type mineralization at Tuscarora might be associated with the Mount Neva intrusive episode, the major intrusive period at Tuscarora, which also generated the Tuscarora epithermal deposits.

Acknowledgments

We thank David John, Bob McCusker, Alan Wallace, Jeff Hedenquist, and Jim Sanborn for information and discussions about volcanic geology, ore deposits, fluid inclusions, and mining history at Tuscarora, and we thank Simon Poulson for S isotope analyses of the three igneous rocks. Geologic mapping was supported by the U.S. Geological Survey (Agreement 1434-HQ-97-AG-01766 [STATEMAP] and Agreement 1434-94-A-1025, Amendment 5 [Mineral Resources Program]), Newcrest Resources, Inc., and Homestake Mining Company. $^{40}\text{Ar}/^{39}\text{Ar}$ ages were determined by CDH in the geochronology laboratory of the New Mexico Bureau of Mines and Mineral Resources, under the guidance of Rich Esser and Lisa Peters. Chemical analyses of altered or mineralized rocks (Table 5) were funded by the Mineral Resources Program of the U.S. Geological Survey. We thank Barney Berger, Eric Struhsacker, David John, Peter Vikre, John Dilles, and Mark Hannington for helpful reviews.

REFERENCES

- Arehart, G.B., 1996, Characteristics and origin of sediment-hosted gold deposits: A review: *Ore Geology Reviews*, v. 11, p. 383–403.
- Arehart, G.B., Foland, K.A., Naeser, C.W., and Kesler, S.E., 1993, $^{40}\text{Ar}/^{39}\text{Ar}$, K-Ar, and fission-track geochronology of sediment-hosted disseminated gold deposits at Post/Betze, Carlin trend, northeastern Nevada: *ECONOMIC GEOLOGY*, v. 88, p. 622–646.
- Ashley, R.P., 1991, The Tonopah precious-metal district, Esmeralda and Nye Counties, Nevada: U.S. Geological Survey Bulletin 1857-H, p. H8–H13.
- Babcock, R.C., Jr., Ballantyne, G.H., and Phillips, C.H., 1995, Summary of the geology of the Bingham district, Utah, in Pierce, F.W., and Bolm, J.G., eds., Porphyry copper deposits of the American Cordillera: *Arizona Geological Society Digest*, v. 20, p. 316–335.
- Berger, B.R., Ridley, W.L., and Tingley, J.V., 1991, Interrelationship of mineralization, volcanism, and tectonism, northern Tuscarora Mountains, Elko County, Nevada, in Thorman, C.H., ed., Some current research in eastern Nevada and western Utah: U.S. Geological Survey Open-File Report 91-386, p. 13–19.
- Bethke, P.M., 1988, The Creede ore-forming system: A summary model: U.S. Geological Survey Open-File Report 88-403, 29 p.
- Black, J.E., Mancuso, T.K., and Gant, J.L., 1991, Geology and mineralization at the Rawhide Au-Ag deposit, Mineral County, Nevada, in Raines, G.L., Lisle, R.E., Schafer, R.W., and Wilkinson, W.H., eds., *Geology and Ore Deposits of the Great Basin: Geological Society of Nevada Symposium*, Reno, 1991, Proceedings, p. 1123–1144.
- Boden, D.R., Struhsacker, E.M., and Wright, B.A., 1993, Structurally controlled volcanism and contrasting types of mineralization, Tuscarora mining district and vicinity, Nevada [abs.]: *Geological Society of America Abstracts with Programs*, v. 25, no. 6, p. 11.
- Bodnar, R.J., and Vityk, M.O., 1994, Interpretation of microthermometric data for H_2O -NaCl fluid inclusions, in De Vivo, B., and Frezzotti, M.L., eds., *Fluid inclusions in minerals: Methods and applications: Short Course of the Working Group (IMA) "Inclusions in Minerals," Pontignano, Siena, Italy*, p. 117–130.
- Bodnar, R.J., Reynolds, T.J., and Kuehn, C.A., 1985, Fluid-inclusion systematics in epithermal systems, in Berger, B.R., and Bethke, P.M., eds., *Geology and geochemistry of epithermal systems: Reviews in Economic Geology*, v. 2, p. 73–97.
- Brake, S.S., and Romberger, S.B., 2000, Precious metal transport and deposition at the New Savage mine, Comstock lode district, Nevada, in Cluer, J.K., Price, J.G., Struhsacker, E.M., Hardyman, R.F., and Morris, C.L., eds., *Geology and Ore Deposits 2000: The Great Basin and Beyond*, Geological Society of Nevada Symposium, Reno, Proceedings, p. 177–186.
- Brooks, J.W., Meinert, L.D., Kuyper, B.A., and Lane, M.L., 1991, Petrology and geochemistry of the McCoy gold skarn, Lander County, Nevada, in Raines, G.L., Lisle, R.E., Schafer, R.W., and Wilkinson, W.H., eds., *Geology and Ore Deposits of the Great Basin: Geological Society of Nevada Symposium*, Reno, 1991, Proceedings, p. 419–442.
- Brooks, W.E., Thorman, W.E., and Snee, L.W., 1995a, The $^{40}\text{Ar}/^{39}\text{Ar}$ r ages and tectonic setting of the middle Eocene northeast Nevada volcanic field: *Journal of Geophysical Research*, v. 100, p. 10,403–10,416.
- Brooks, W.E., Thorman, W.E., Snee, L.W., Nutt, C.W., Potter, C.J., and Dubiel, R.F., 1995b, Summary of chemical analyses and $^{40}\text{Ar}/^{39}\text{Ar}$ -spectra data for Eocene volcanic rocks from the central part of the northeast Nevada volcanic field: U.S. Geological Survey Bulletin 1988-K, p. K1–K33.
- Carlson, D.H., Fleck, R., Moye, F.J., and Fox, K.F., 1991, Geology, geochemistry, and isotopic character of the Colville igneous complex, north-eastern Washington: *Journal of Geophysical Research*, v. 96, p. 13,313–13,333.
- Cathles, L.M., 1981, Fluid flow and genesis of hydrothermal ore deposits: *ECONOMIC GEOLOGY 75TH ANNIVERSARY VOLUME*, p. 442–457.
- Cathles, L.M., Erendi, A.H.J., and Barrie, T., 1997, How long can a hydrothermal system be sustained by a single intrusive event?: *ECONOMIC GEOLOGY*, v. 92, p. 766–771.
- Christiansen, R.L., and Yeats, R.S., 1992, Post-Laramide geology of the U.S. Cordilleran region, in Burchfiel, B.C., Lipman, P.W., and Zoback, M.L., eds., *The Cordilleran orogen: Conterminous U.S.: Geological Society of America, The Geology of North America*, v. G-3, p. 261–406.
- Clark, T.M., Ehman, K.D., and Axelrod, D.I., 1985, Late Eocene extensional faulting in the northern Basin and Range province, Nevada: *Geological Society of America Abstracts with Programs*, v. 17, no. 6, p. 348.
- Cline, J.S., 2001, Timing of gold and arsenic sulfide mineral deposition at the Getchell Carlin-type gold deposit, north-central Nevada: *ECONOMIC GEOLOGY*, v. 96, p. 75–89.
- Coats, R.R., 1987, *Geology of Elko County, Nevada*: Nevada Bureau of Mines and Geology Bulletin 101, 112 p.
- Crawford, K.S., 1992, *The geology of the Tuscarora mining district, Elko County, Nevada*: Unpublished M.S. thesis, Reno, University of Nevada, 85 p.
- Deino, A., and Potts, R., 1990, Single-crystal $^{40}\text{Ar}/^{39}\text{Ar}$ dating of the Ologesailie Formation, southern Kenya rift: *Journal of Geophysical Research*, v. 95, p. 8453–8470.
- DeWitt, E., Thorson, J.P., and Smith, R.C., 1991, *Geology and gold deposits of the Oatman district, northwestern Arizona*: U.S. Geological Survey Bulletin 1857-I, p. 11–128.
- Emmons, W.H., 1910, *A reconnaissance of some mining camps in Elko, Lander, and Eureka counties, Nevada*: U.S. Geological Survey Bulletin 408, 130 p.
- Emsbo, P., Hofstra, A., Park, D., Zimmerman, J.M., and Snee, L., 1996, A mid-Tertiary age constraint on alteration and mineralization in igneous dikes on the Goldstrike property, Carlin trend, Nevada [abs.]: *Geological Society of America Abstracts with Programs*, v. 28, p. A-476.
- Eng, T., Boden, D.R., Reischman, M.R., and Biggs, J.O., 1996, *Geology and mineralization of the Bullfrog mine and vicinity, Nye County, Nevada*, in Coyner, A.R., and Fahey, P.L., eds., *Geology and Ore Deposits of the American Cordillera: Geological Society of Nevada Symposium*, Reno, 1995, Proceedings, p. 353–402.
- Giesemann, A., Jaeger, H.J., Norman, A.L., Krouse, H.R., and Brand, W.A., 1994, On-line sulfur isotope determination using elemental analyzer coupled to a mass spectrometer: *Analytical Chemistry*, v. 65, p. 2816–2819.
- Goldstein, R.H., and Reynolds, T.J., 1994, *Systematics of fluid inclusions in diagenetic minerals: Society of Sedimentary Geologists Short Course 31*, Tulsa, Oklahoma, SEPM, 199 p.
- Groff, J.A., Heizler, M.T., McIntosh, W.C., and Norman, D.I., 1997, $^{40}\text{Ar}/^{39}\text{Ar}$ dating and mineral paragenesis for Carlin-type gold deposits along the Getchell trend, Nevada: Evidence for Cretaceous and Tertiary gold mineralization: *ECONOMIC GEOLOGY*, v. 92, p. 601–622.
- Haas, J.L., Jr., 1971, The effect of salinity on the maximum thermal gradient of a hydrothermal system at hydrostatic pressure: *ECONOMIC GEOLOGY*, v. 66, p. 940–946.
- Hall, C.M., Simon, G., and Kesler, S.E., 1997, Age of mineralization at the Twin Creeks SHMG deposit, Nevada, in Vikre, P., Thompson, T.B., Bettles, K., Christensen, O., and Parratt, R., eds., *Carlin-type gold deposits field conference: Society of Economic Geologists Guidebook Series*, v. 28, p. 151–154.
- Hall, C.M., Kesler, S.E., Simon, G., and Fortuna, J., 2000, Overlapping Cretaceous and Eocene alteration, Twin Creeks Carlin-type deposit: *ECONOMIC GEOLOGY*, v. 95, p. 1739–1752.
- Hasler, R.W., Wilson, W.R., and Darnton, B.T., 1991, *Geology and ore deposits of the Ward mining district, White Pine County, Nevada*, in Raines, G.L., Lisle, R.E., Schafer, R.W., and Wilkinson, W.H., eds., *Geology and*

- Ore Deposits of the Great Basin: Geological Society of Nevada Symposium, Reno, 1991, Proceedings, p. 333–353.
- Heald, P., Foley, N.K., and Hayba, D.O., 1987, Comparative anatomy of volcanic-hosted epithermal deposits: Acid-sulfate and adularia-sericite types: *ECONOMIC GEOLOGY*, v. 82, p. 1–26.
- Hedenquist, J.W., and Henley, R.W., 1985, Hydrothermal eruptions in the Waiotapu geothermal system, New Zealand—Their origin, associated breccias, and relation to precious metal mineralization: *ECONOMIC GEOLOGY*, v. 80, p. 1640–1668.
- Hedenquist, J.W., and Lowenstern, J.B., 1994, The role of magmas in the formation of hydrothermal ore deposits: *Nature*, v. 370, p. 519–527.
- Hedenquist, J.W., Reyes, A.G., Simmons, S.F., and Taguchi, S., 1991, The thermal and geochemical structure of active and fossil epithermal systems deduced from fluid inclusion studies, in *European current research on fluid inclusions XI: Plinius (Italian supplement to European Journal of Mineralogy)*, Dipartimento di Scienze della Terra, Milano, Italy, Abstracts, p. 98–99.
- 1992, The thermal and geochemical structure of geothermal and epithermal systems: A framework for interpreting fluid inclusion data: *European Journal of Mineralogy*, v. 4, p. 989–1015.
- Henry, C.D., and Boden, D.R., 1998a, Geologic map of the Mount Blitzen Quadrangle, Elko County, northeastern Nevada: Nevada Bureau of Mines and Geology Map 110, scale 1:24,000 (20 p.).
- 1998b, Eocene magmatism: The heat source for Carlin-type gold deposits of northern Nevada: *Geology*, v. 26, p. 1067–1070.
- 1999, Geologic map of the southern part of the Toe Jam Mountain Quadrangle, Nevada: Nevada Bureau of Mines and Geology Map 117, scale 1:24,000, 12 p. text.
- Henry, C.D., and Ressel, M.W., 2000, Eocene magmatism—The smoking gun for Carlin-type deposits, in Cluer, J.K., Price, J.G., Struhsacker, E.M., Hardyman, R.F., and Morris, C.L., eds., *Geology and Ore Deposits 2000: The Great Basin and Beyond: Geological Society of Nevada Symposium*, Reno, 2000, Proceedings, v. 1, p. 365–388.
- Henry, C.D., Elson, H.B., McIntosh, W.C., Heizler, M.T., and Castor, S.B., 1997, Brief duration of hydrothermal activity at Round Mountain, Nevada, determined from $^{40}\text{Ar}/^{39}\text{Ar}$ geochronology: *ECONOMIC GEOLOGY*, v. 92, p. 807–826.
- Henry, C.D., Boden, D.R., and Castor, S.B., 1998, Geology and mineralization of the Eocene Tuscarora volcanic field, Elko County, Nevada, in Tosdal, R.M., ed., *Contributions to the Au metallogeny of northern Nevada*, U.S. Geological Survey Open-File Report 98-338, p. 279–290.
- Henry, C.D., Boden, D.R., and Castor, S.B., 1999, Geologic map of the Tuscarora Quadrangle, Nevada: Nevada Bureau of Mines and Geology Map 116, scale 1:24,000, 20 p. text.
- Henry, C.D., Faulds, J.E., Boden, D.R., and Ressel, M.W., 2001, Timing and styles of Cenozoic extension near the Carlin trend, northeastern Nevada: Implications for the formation of Carlin-type gold deposits: *Geological Society of Nevada Special Publication* 33, p. 115–128.
- Hildenbrand, T.G., and Kucks, R.P., 1988, Total intensity magnetic anomaly map of Nevada: Nevada Bureau of Mines and Geology Map 93A, scale 1:750,000.
- Hiza, M.M., and Grunder, A.L., 1997, Geochemical, isotopic, and mineralogical variability of Eocene alkaline magmatism: Absaroka volcanic province, USA [abs.]: *Geological Society of America Abstracts with Programs*, v. 29, no. 6, p. A-87.
- Hofstra, A.H., 1994, Geology and genesis of the Carlin-type gold deposits in the Jerritt Canyon district, Nevada: Unpublished Ph.D. dissertation, Boulder, University of Colorado, 719 p.
- 1997, Isotopic composition of sulfur in Carlin-type gold deposits: Implications for genetic models, in Vikre, P., Thompson, T.B., Bettles, K., Christensen, O., and Parratt, R., eds., *Carlin-type gold deposits field conference: Society of Economic Geologists Guidebook Series*, v. 28, p. 119–129.
- Hofstra, A.H., and Cline, J.S., 2000, Characteristics and models for Carlin-type gold deposits: *Reviews in Economic Geology*, v. 13, p. 163–220.
- Hofstra, A.H., Snee, L.W., Rye, R.O., Folger, H.W., Phinisey, J.D., Loranger, R.J., Dahl, A.R., Naeser, C.W., Stein, H.J., and Lewchuk, M., 1999, Age constraints on Jerritt Canyon and other Carlin-type gold deposits in the western United States—Relationship to mid-Tertiary extension and magmatism: *ECONOMIC GEOLOGY*, v. 94, p. 769–802.
- Hooper, P.R., Bailey, D.G., and McCarley Holder, G.A., 1995, Tertiary calc-alkaline magmatism associated with lithospheric extension in the Pacific Northwest: *Journal of Geophysical Research*, v. 100, p. 10,303–10,319.
- Ilchik, R.P., and Barton, M.D., 1997, An amagmatic origin of Carlin-type gold deposits: *ECONOMIC GEOLOGY*, v. 92, p. 269–288.
- Janecke, S.U., Hammond, B.F., Snee, L.W., and Geissman, J.W., 1997, Rapid extension in an Eocene volcanic arc: Structure and paleogeography of an intra-arc half graben in central Idaho: *Geological Society of America Bulletin*, v. 109, p. 253–267.
- John, D.A., 2001, Miocene and early Pliocene epithermal gold-silver deposits in the northern Great Basin, western United States: Characteristics, distribution, and relationship to magmatism: *ECONOMIC GEOLOGY*, v. 96, p. 1827–1853.
- John, D.A., and Wallace, A.R., 2000, Epithermal gold-silver deposits related to the northern Nevada rift, in Cluer, J.K., Price, J.G., Struhsacker, E.M., Hardyman, R.F., and Morris, C.L., eds., *Geology and Ore Deposits 2000: The Great Basin and Beyond: Geological Society of Nevada Symposium*, Reno, 2000, Proceedings, p. 155–175.
- John, D.A., Garside, L.J., and Wallace, A.R., 1999, Magmatic and tectonic setting of late Cenozoic epithermal gold-silver deposits in northern Nevada, with an emphasis on the Pah Rah and Virginia Ranges and the northern Nevada rift, in Kizis, J.A., ed., *Low-sulfidation gold deposits in northern Nevada: Geological Society of Nevada Special Publication* 29, p. 65–158.
- Johnston, M.K., 2000, Hypogene alteration and ore characteristics at the Cove gold-silver deposit, Lander County, Nevada, in Cluer, J.K., Price, J.G., Struhsacker, E.M., Hardyman, R.F., and Morris, C.L., eds., *Geology and Ore Deposits 2000: The Great Basin and Beyond: Geological Society of Nevada Symposium*, Reno, 2000, Proceedings, p. 621–641.
- LaPointe, D.D., Tingley, J.V., and Jones, R.B., 1991, Mineral resources of Elko County, Nevada: Nevada Bureau of Mines and Geology Bulletin 106, 236 p.
- Leonardson, R.W., and Rahn, J.E., 1996, Geology of the Betze-Post gold deposits, Eureka County, Nevada, in Coyner, A.R., and Fahey, P.L., eds., *Geology and Ore Deposits of the American Cordillera: Geological Society of Nevada Symposium*, Reno, 1996, Proceedings, p. 61–94.
- Lipman, P.W., 1992, Ash-flow calderas as structural controls of ore deposits—Recent work and future problems, in Thorman, C. H., ed., *Application of structural geology to mineral and energy resources of the central and western United States: U.S. Geological Survey Bulletin* 2012, p. L1–L12.
- Marsh, T.M., Einaudi, M.T., and McWilliams, Michael, 1997, $^{40}\text{Ar}/^{39}\text{Ar}$ geochronology of Cu-Au and Au-Ag mineralization in the Portrerillos district, Chile: *ECONOMIC GEOLOGY*, v. 92, p. 784–806.
- McCarley Holder, G.A., Holder, R.W., and Carlson, D.H., 1990, Middle Eocene dike swarms and their relation to contemporaneous plutonism, volcanism, core-complex mylonitization, and graben subsidence, Okanogan Highlands, Washington: *Geology*, v. 18, p. 1082–1085.
- McIntosh, W.C., and Chamberlin, R.M., 1994, $^{40}\text{Ar}/^{39}\text{Ar}$ geochronology of middle to late Cenozoic ignimbrites, mafic lavas, and volcaniclastic rocks in the Quemado region, New Mexico: *New Mexico Geological Society Guidebook*, v. 45, p. 165–185.
- McIntyre, D.H., Ekren, E.B., and Hardyman, R.F., 1982, Stratigraphic and structural framework of the Challis volcanics in the eastern half of the Challis 1° by 2° Quadrangle, Idaho, in Bonnicksen, B., and Breckenridge, R.M., eds., *Cenozoic geology of Idaho: Idaho Bureau of Mines and Geology Bulletin* 26, p. 3–22.
- Nash, J.T., Utterback, W.C., and Trudel, W.S., 1995, Geology and geochemistry of Tertiary volcanic host rocks, Sleeper gold-silver deposit, Humboldt County, Nevada: *U.S. Geological Survey Bulletin* 2090, 63 p.
- Nolan, T.B., 1936, The Tuscarora mining district, Elko County, Nevada: *University of Nevada Bulletin*, v. 30 and *Nevada Bureau of Mines and Geology Bulletin* 25, 36 p.
- Ohmoto, H., and Rye, R.O., 1979, Isotopes of sulfur and carbon, in Barnes, H.L., ed., *Geochemistry of hydrothermal ore deposits—second edition: New York, Wiley*, p. 509–567.
- Phinisey, J.D., Hofstra, A.H., Snee, L.W., Roberts, T.T., Dahl, A.R., and Loranger, R.J., 1996, Evidence for multiple episodes of igneous and hydrothermal activity and constraints on the timing of gold mineralization, Jerritt Canyon district, Elko County, Nevada, in Coyner, A.R., and Fahey, P.L., eds., *Geology and Ore Deposits of the American Cordillera: Geological Society of Nevada Symposium*, Reno, 1996, Proceedings, p. 15–39.
- Reed, M.H., 1998, Calculation of simultaneous chemical equilibria in aqueous-mineral-gas systems and its application to modeling hydrothermal processes, in *Techniques in hydrothermal ore deposits geology: Reviews in Economic Geology*, v. 10, p. 109–124.
- Ressel, M.W., Noble, D.C., Henry, C.D., and Trudel, W.S., 2000a, Dike-hosted ores of the Beast deposit and the importance of Eocene magmatism

- in gold mineralization of the Carlin trend, Nevada: *ECONOMIC GEOLOGY*, v. 95, p. 1417–1444.
- Ressel, M.W., Noble, D.C., Volk, J.A., Lamb, J.B., Park, D.E., Conrad, J.E., Heizler, M.T., and Mortensen, J.K., 2000b, Precious-metal mineralization in Eocene dikes at Griffin and Meikle: Bearing on the age and origin of gold deposits of the Carlin trend, Nevada, in Cluer, J.K., Price, J.G., Struhsacker, E.M., Hardyman, R.F., and Morris, C.L., eds., *Geology and Ore Deposits 2000, The Great Basin and Beyond: Geological Society of Nevada Symposium, Reno, 2000, Proceedings*, p. 79–101.
- Ressel, M.W., Noble, D.C., Henry, C.D., and Trudel, W.S., 2001, Dike-hosted ores of the Beast deposit and the importance of Eocene magmatism in gold mineralization of the Carlin trend, Nevada—reply: *ECONOMIC GEOLOGY*, v. 96, p. 666–668.
- Robbins, C.H., 2000, Geology of the El Peñon gold-silver deposit, northern Chile, in Cluer, J.K., Price, J.G., Struhsacker, E.M., Hardyman, R.F., and Morris, C.L., eds., *Geology and Ore Deposits 2000: The Great Basin and Beyond: Geological Society of Nevada Symposium, Reno, 2000, Proceedings*, p. 249–264.
- Roberts, R.J., 1964, Stratigraphy and structure of the Antler Peak Quadrangle, Humboldt and Lander counties, Nevada: U.S. Geological Survey Professional Paper 459-A, 93 p.
- Samson, S.D., and Alexander, E.C., Jr., 1987, Calibration of the interlaboratory $^{40}\text{Ar}/^{39}\text{Ar}$ dating standard, MMhb-1: *Chemical Geology*, v. 66, p. 27–34.
- Sander, M.V., and Einaudi, M.T., 1990, Epithermal deposition of gold during transition from propylitic to potassic alteration at Round Mountain, Nevada: *ECONOMIC GEOLOGY*, v. 85, p. 285–311.
- Sasaki, A., Arikawa, Y., and Folinsbee, R.E., 1979, Kiba reagent method of sulfur extraction applied to isotopic work: *Bulletin of the Geological Survey of Japan*, v. 30, p. 241–245.
- Seedorff, E., 1991, Magmatism, extension, and ore deposits of Eocene to Holocene age in the Great Basin—Mutual effects and preliminary proposed genetic relationships, in Raines, G.L., Lisle, R.E., Schafer, R.W., and Wilkinson, W.H., eds., *Geology and Ore Deposits of the Great Basin: Geological Society of Nevada Symposium, Reno, 1991, Proceedings*, p. 133–178.
- Seward, T.M., 1989, The hydrothermal chemistry of gold and its implications for ore formation: Boiling and conductive cooling as examples, in Keays, R.R., Ramsay, W.R.H., and Groves, D.I., eds., *The Geology of gold deposits: The Perspective in 1988: ECONOMIC GEOLOGY MONOGRAPH 6*, p. 398–404.
- Sillitoe, R.H., and Bonham, H.F., Jr., 1990, Sediment-hosted gold deposits: Distal products of magmatic-hydrothermal systems: *Geology*, v. 18, p. 157–161.
- Simmons, S.F., 1991, Hydrologic implications of alteration and fluid inclusion studies in the Fresno district, Mexico: Evidence for a brine reservoir and a descending water table during the formation of hydrothermal Ag-Pb-Zn orebodies: *ECONOMIC GEOLOGY*, v. 86, p. 1579–1601.
- Simmons, S.F., and Browne, P.R.L., 2000, Mineral indicators of boiling in modern low-sulfidation epithermal environments, Broadlands-Ohaaki and Waiotapu geothermal systems, New Zealand [abs.]: *Geology and Ore Deposits 2000: The Great Basin and Beyond, Geological Society of Nevada Symposium, Reno, 2000, Program with Abstracts*, p. 75–76.
- Simmons, S.F., and Christenson, B.W., 1994, Origins of calcite in a boiling geothermal system: *American Journal of Science*, v. 294, p. 361–400.
- Smith, D.M., Jr., Albinson, T., and Sawkins, F.J., 1982, Geology and fluid inclusion studies of the Tayoltita silver-gold vein deposits, Durango, Mexico: *ECONOMIC GEOLOGY*, v. 77, p. 1120–1145.
- Snoke, A.W., Howard, K.A., McGrew, A.J., Burton, B.R., Barnes, C.G., Peters, M.T., and Wright, J.E., 1997, The grand tour of the Ruby-East Humboldt metamorphic core complex, northeastern Nevada: *Brigham Young University Geological Studies*, v. 42, p. 1, p. 225–269.
- Spycher, N.F., and Reed, M.H., 1989, Evolution of a Broadlands-type epithermal ore fluid along alternative P-T paths—Implications for the transport and deposition of base, precious, and volatile metals: *ECONOMIC GEOLOGY*, v. 84, p. 328–359.
- Steiger, R.H., and Jäger, E., 1977, Subcommittee on geochronology: Convention on the use of decay constants in geo- and cosmochronology: *Earth and Planetary Science Letters*, v. 36, p. 359–362.
- Stewart, J.H., and Carlson, J.E., 1978, Geologic map of Nevada: U.S. Geological Survey in collaboration with Nevada Bureau of Mines and Geology, scale 1:500,000.
- Teal, L., and Jackson, M., 1997, Geologic overview of the Carlin trend gold deposits and descriptions of recent deep discoveries: *Society of Economic Geologists Newsletter*, no. 31, p. 1, 13–25.
- Theodore, T.G., 2000, Geology of pluton-related gold mineralization at Battle Mountain, Nevada: *Center for Mineral Resources, Tucson, Arizona, Monographs in Mineral Resource Science 2*, 271 p.
- Thorman, C.H., Brooks, W.E., Snee, L.W., Hofstra, A.H., Christensen, O.D., and Wilton, D.T., 1995, Eocene-Oligocene model for Carlin-type deposits in northern Nevada, in Coyner, A.R., and Fahey, P.L., eds., *Geology and Ore Deposits of the American Cordillera: Geological Society of Nevada Symposium, Reno, 1995, Proceedings*, p. 75.
- Tosdal, R.M., Cline, J.S., Hofstra, A.H., Peters, S.G., Wooden, J.L., and Young-Mitchell, M.N., 1998, Mixed sources of Pb in sedimentary-rock-hosted Au deposits, northern Nevada, in Tosdal, R.M., ed., *Contributions to the Au metallogeny of northern Nevada: U.S. Geological Survey Open-File Report 98-338*, p. 223–233.
- Tosdal, R.M., Wooden, J.L., and Kistler, R.W., 2000, Geometry of the Neoproterozoic continental breakup, and implications for location of Neovadan mineral belts, in Cluer, J.K., Price, J.G., Struhsacker, E.M., Hardyman, R.F., and Morris, C.L., eds., *Geology and Ore Deposits 2000, The Great Basin and Beyond: Geological Society of Nevada Symposium, Reno, 2000, Proceedings*, p. 451–466.
- Tretbar, D.R., Arehart, G.B., and Christensen, J.N., 2000, Dating gold deposition in a Carlin-type gold deposit using Rb/Sr methods on the mineral galkhaite: *Geology*, v. 28, p. 947–950.
- Vikre, P.G., 1985, Precious metal vein systems in the National district, Humboldt County, Nevada: *ECONOMIC GEOLOGY*, v. 80, p. 360–393.
- 1989, Fluid-mineral relations in the Comstock lode: *ECONOMIC GEOLOGY*, v. 84, p. 1574–1613.
- Westra, G., and Riedell, K.B., 1996, Geology of the Mount Hope stockwork molybdenum deposit, Eureka County, Nevada, in Coyner, A.R., and Fahey, P.L., eds., *Geology and Ore Deposits of the American Cordillera: Geological Society of Nevada Symposium, Reno, 1996, Proceedings*, p. 1639–1666.
- White, N.C., and Hedenquist, J.W., 1995, Epithermal gold deposits: Styles, characteristics, and exploration: *Society of Economic Geologists Newsletter*, no. 23, p.1, 9–13.
- Whitehill, H.R., 1876, Nevada State Mineralogist Biennial Report, 1874–1875.
- 1878, Nevada State Mineralogist Biennial Report, 1876–1877.
- Wooden, J.L., Kistler, R.W., and Tosdal, R.M., 1998, Pb isotopic mapping of crustal structure in the northern Great Basin and relationships to Au deposit trends, in Tosdal, R.M., ed., *Contributions to the Au metallogeny of northern Nevada: U.S. Geological Survey Open-File Report 98-338*, p. 20–33.